NAVAL POSTGRADUATE SCHOOL
Monterey, California

THESIS

THE INTERACTION OF A FLUID INTERFACE WITH A VORTEX PAIR

by

Mark D. Petersen-Overton

June 1988

Thesis Advisor: T. Sarpkaya

Approved for public release; distribution is unlimited.

UNCLASSIFIED
SECURITY CLASSIFICATION OF THIS PAGE

REPORT DOCUMENTATION PAGE

1a REPORT SECURITY CLASSIFICATION UNCLASSIFIED	1b RESTRICTIVE MARKINGS
2a SECURITY CLASSIFICATION AUTHORITY 2b DECLASSIFICATION / DOWNGRADING SCHEDULE	3 DISTRIBUTION / AVAILABILITY OF REPORT Approved for public release; distribution is unlimited
4 PERFORMING ORGANIZATION REPORT NUMBER(S)	5 MONITORING ORGANIZATION REPORT NUMBER(S)
6a NAME OF PERFORMING ORGANIZATION Naval Postgraduate school 6b OFFICE SYMBOL (If applicable)	7a NAME OF MONITORING ORGANIZATION Naval Postgraduate school
6c ADDRESS (City, State, and ZIP Code) Monterey, California 93943-5000	7b ADDRESS (City, State, and ZIP Code) Monterey, California 93943-5000
8a NAME OF FUNDING, SPONSORING ORGANIZATION 8b OFFICE SYMBOL (If applicable)	9 PROCUREMENT INSTRUMENT IDENTIFICATION NUMBER
8c ADDRESS (City, State, and ZIP Code)	10 SOURCE OF FUNDING NUMBERS PROGRAM ELEMENT NO / PROJECT NO / TASK NO / WORK UNIT ACCESSION NO

11 TITLE (Include Security Classification)

THE INTERACTION OF A FLUID INTERFACE WITH A VORTEX PAIR

12 PERSONAL AUTHOR(S)
Petersen-Overton, Mark D.

13a TYPE OF REPORT	13b TIME COVERED	14 DATE OF REPORT (Year, Month, Day)	15 PAGE COUNT
Master's Thesis	FROM _____ TO _____	1988 June	76

16 SUPPLEMENTARY NOTATION The views in this thesis are those of the author and do not reflect the official policy or position of the department of defense or the U.S. Government

17 COSATI CODES			18 SUBJECT TERMS (Continue on reverse if necessary and identify by block number)
FIELD	GROUP	SUB-GROUP	Trailing Vortices Sinusoidal Instability

19 ABSTRACT (Continue on reverse if necessary and identify by block number)

A detailed parametric study of the variables critical to a numerical model of the interaction of a free surface with an ascending vortex pair has been carried out. The model is based on a discrete vortex representation of the free surface and the use of the appropriate boundary conditions. A study was performed to minimize the numerical Helmholtz instabilities inherent in the numerical model for lower Froude numbers. A method of free-surface re-discretization was developed and implemented. Additionally, an investigation of the motion of a vortex pair approaching and passing through a sharp salt/freshwater density interface was conducted. Experiments were performed in a large basin and the vortices were generated with two counter-rotating plates. The rise and intrusion of the Kelvin oval into the upper layer of lower density fluid was recorded on a video tape and then analyzed through the use of a motion analysis system.

20 DISTRIBUTION / AVAILABILITY OF ABSTRACT	21 ABSTRACT SECURITY CLASSIFICATION
XX UNCLASSIFIED/UNLIMITED ☐ SAME AS RPT ☐ DTIC USERS	UNCLASSIFIED
22a NAME OF RESPONSIBLE INDIVIDUAL Prof. T. Sarpkaya	22b TELEPHONE (Include Area Code) (408) 646-3425 / 22c OFFICE SYMBOL Code 69Si

DD FORM 1473, 84 MAR 83 APR edition may be used until exhausted
All other editions are obsolete

SECURITY CLASSIFICATION OF THIS PAGE

☆ U.S. Government Printing Office 1986—606-243

UNCLASSIFIED

Approved for public release; distribution is unlimited

The Interaction of a Fluid Interface with a Vortex Pair

by

Mark D. Petersen-Overton
Lieutenant, United States Navy
B.S., University of South Carolina, 1978

Submitted in partial fulfillment of the
requirements for the degree of

MASTER OF SCIENCE IN MECHANICAL ENGINEERING

from the

NAVAL POSTGRADUATE SCHOOL
June 1988

ABSTRACT

A detailed parametric study of the variables critical to a numerical model of the interaction of a free surface with an ascending vortex pair has been carried out. The model is based on a discrete vortex representation of the free surface and the use of the appropriate boundary conditions. A study was performed to minimize the numerical Helmholtz instabilities inherent in the numerical model for lower Froude numbers. A method of free-surface re-discretization was developed and implemented. Additionally, an investigation of the motion of a vortex pair approaching and passing through a sharp salt/freshwater density interface was conducted. Experiments were performed in a large basin and the vortices were generated with two counter-rotating plates. The rise and intrusion of the Kelvin oval into the upper layer of lower density fluid was recorded on a video tape and then analyzed through the use of a Motion Analysis system.

TABLE OF CONTENTS

LIST OF FIGURES

TABLE OF SYMBOLS AND ABBREVIATIONS

b_0	Initial vortex pair spacing
N	Number of discrete free surface vortices
d_0	Initial depth of the vortex pair
Fr	Froude Number
g	Gravitational acceleration
i	$\sqrt{-1}$
q_m	Scalar velocity $\sqrt{u^2+v^2}$
t	Time
T*	Nondimensional time $\frac{V_0 t}{b_0}$
u	X-component of velocity
v	Y-component of velocity
V_0	Initial or steady state mutual induction velocity
V*	Nondimensional velocity $\frac{V}{V_0}$
w(z)	Complex velocity function
x	Horizontal component of the coordinate axis (parallel to the line joining the vortex cores)
y	Vertical component of the coordinate axis
z_i	Complex position of a vortex

z_0	Complex position of the right-hand vortex in the vortex pair
$\bar{z}_i$	Complex conjugate of z_i
$\bar{z}_0$	Complex conjugate of z_0
δ	De-singularization parameter
Γ_N	Circulation of a given distributed vortex
Γ_0	Circulation of the vortex pair
η	Position of the free surface
η_m	$\frac{\eta}{L_c}$
ϕ	Velocity potential
ϕ_m	$\frac{\phi}{\Gamma_0}$
xmax	The maximum x/b_o position along the free surface
xv	The x/bo position of the center of the free surface vortex distribution
Znew	Complex position of an added free surface vortex element
Vnew	New vortex added to free surface
Γnew	Value of circulation assigned to an added free surface vortex
$\Delta\rho$	Difference in density between the salt and fresh water layer
ρ_s	Density of salt water layer
C	Concentration of salt layer

ACKNOWLEDGMENTS

The author wishes to express his sincere appreciation to Distinguished Professor T. Sarpkaya for his inspiration and assistance throughout this research effort and for ensuring that the thesis work was an *educational experience*. The author would also like to thank LT Richard E. Leeker for his invaluable help during the first several months of this work. Appreciation is also extended to Mr. Jack McKay, who always seemed to be at the right place at the right time, ready to extend his helping hand.

I. INTRODUCTION

The understanding of the temporal development of the surface signatures resulting from the interaction of an ascending inclined vortex pair with the free surface is of special importance. When a trailing vortex pair, generated by a lifting surface, approaches the free surface, with or without mutual induction instability and/or vortex breakdown, the vortices and/or the crude vortex rings give rise to surface disturbances (scars and striations). The striations are essentially three-dimensional free-surface disturbances, normal to the direction of the motion of the lifting surface, and come into existence when the vortex pair is at a distance equal to about one initial vortex separation from the free surface. The scars are small free-surface depressions on either side of a nearly symmetrical hump, directly above the plane of symmetry of the vortex pair. They come into existence towards the end of the pure striation phase and when the vortices are at a distance equal to about 60 percent of the initial vortex separation from the free surface. The scars are created and driven by the vortices and both move outward. Subsequently, the vortices diffuse rapidly and their circulation decreases slowly at first (prior to the occurrence of scars) and rapidly thereafter due to the counter-sign vorticity generated in the overlapping regions of the vortex pair in the recirculation cell and at the free surface.

The surface disturbances or the local roughening of the free surface, resulting from the vortex motion produced by submerged foils or counter-rotating propellers, are visible because the particle motions they create as they propagate produce a straining field at the surface which modifies the physical characteristics of the sea surface (reflection, refraction, and the scattering of sound, heat, and light). In fact, in many photographs of the sea surface taken from aircraft or earth resources technology satellites, using passive or active sensors, the differential roughening of the free surface can be seen clearly.

Previous studies of a vortex (or vortex pair) in ground- or free-surface effect have been generally concerned with the boundary layer development, generation of oppositely-signed vorticity, the flow resulting from a single vortex held fixed in a uniform flow and the so-called "rebounding" phenomenon, according to which the vortices move at first toward the boundary, as on an inviscid trajectory, and then away from it. The boundary surface may be either a rigid boundary at which the no-slip condition is satisfied or a free surface corresponding to zero shear stress. In either case, the boundary surface (sometimes erroneously referred to as a vorticity sink) gives rise to oppositely signed vorticity and the net circulation of the vortices decreases with time.

The interaction of vortices with a fluid interface has been under investigation at the Naval Postgraduate School by Sarpkaya and his students for the past several years [Refs. 1–11]. The emphasis of these

investigations has been the identification of the specific mechanisms which lead to the demise of the vortices and the prediction, through experiments and analysis, of the motion of vortices and the form of the free surface.

Sarpkaya and Henderson's [Ref. 9] theoretical analysis of the scars created by the trailing vortices was carried out assuming the vortices to be two-dimensional and the free surface to be a rigid plane. For small Froude numbers $\left(Fr = V_0/\sqrt{gb_0}\right)$, (where V_0 is the initial mutual induction velocity of the vortices and b_0 is the initial vortex separation), each scar front was shown to coincide with the stagnation point on the Kelvin oval, formed by one of the pair of the trailing vortices and its image. For Froude numbers larger than about 0.15, not only the deformation of the free surface but also the nonlinear interaction between the said deformation and the motion of the vortices is significant. Thus, the free surface may no longer be assumed rigid. However, the analysis of a three-dimensional interaction between the surface and the inclined vortex pair is extremely difficult. It is in view of this fact that it was decided to generate nearly two-dimensional vortex pairs at relatively high Froude numbers and to carry out a numerical analysis assuming a deformable free surface. Most recently, Leeker [Ref. 11] continued the work on the interaction of a vortex pair with the free surface. His task was to improve upon the discrete vortex model, originally constructed by Elnitsky [Ref 10], by reducing or eliminating the numerical instabilities present at lower Froude numbers. This improvement

would enable the model to more closely represent the results observed in the laboratory by allowing the calculations to progress further in time.

The present investigation has a two-fold purpose:

1. To conduct a detailed parametric study of the variables affecting the performance of the discrete vortex model and identify the variables (if any) that adversely or positively affect the performance of the model with particular emphasis on their effects on observed numerical instabilities. Once it has been determined how sensitive the numerical model is to a variety of variables, efforts are made to attempt a qualitative optimization of these variables under specific conditions. Armed with the information gained in the parametric study, additional efforts are made to obtain methods that remove or neutralize numerical instabilities present at lower Froude numbers. Several smoothing techniques and re-discretization schemes are attempted.

2. To investigate the motion of a vortex pair approaching and intruding through a sharp density interface. Utilizing an improved test apparatus and a sharp salt/fresh water interface, a complete investigation was conducted to analyze the interaction of the vortices and the Kelvin oval with the interface. The motion of the vortex centers was recorded on video tape and analyzed through the use of a motion analysis system.

II. PARAMETRIC STUDY OF THE NUMERICAL MODEL

A. INTRODUCTION

The discrete vortex model used in this investigation and in the previous work is discussed by Elnitsky and Leeker in detail [Refs. 10, 11]. In summary, discrete vortices are placed along the free surface to form a vortex sheet. The inter-vortex spacing may vary as desired, emanating from a pre-selected center of vortex distribution along the free surface. After the program is executed, each individual surface vortex is convected utilizing the velocities imparted to it by all other vortices and the main rising vortex pair. Execution continues until numerical Helmholtz instabilities develop and chaos ensues.

The complex function representing all of the vortices in the system is given by:

$$w = -\frac{\ln(z - z_o)}{2i\pi} - \frac{\ln(z + \bar{z}_o)}{2i\pi} - \sum_{k=1}^{m} \frac{\Gamma_k \ln(z - z_k)}{2i\pi} + \sum_{k=1}^{m} \frac{\Gamma_k \ln(z + \bar{z}_k)}{2i\pi} \quad (1)$$

The strengths of the free-surface vortices are normalized by the strength of the main vortex. Spatial units are normalized by the distance b_0, the initial spacing between the two main vortex centers. Velocities are normalized by $V_0 = \Gamma_0 / 2b_0$ and time is normalized by $T^* = V_0 t / b_0$.

The normalized boundary condition at the free surface is then given by:

$$\frac{D\phi_m}{DT^*} - \frac{q_m^2}{2} + \frac{\eta_m}{Fr^2} = 0 \qquad (2)$$

and the induced velocity becomes:

$$\frac{dw}{dt} = u - iv = -\frac{i}{2\pi(z-z_0)} + \frac{i}{2\pi(z+\bar{z}_0)} + \sum_{k=1}^{m}\frac{i\Gamma_m}{2\pi(z-z_i)} - \sum_{k=1}^{m}\frac{i\Gamma_m}{2\pi(z+\bar{z}_i)} \qquad (3)$$

There are other numerical methods available to solve the problem of the interaction of a free surface with a vortex pair, and Elnitsky discusses them in great detail [Ref 10]. The principal advantages of the Boundary Integral Equation method utilized in this and preceding investigations are the ability to discretize the free surface without a loss of accuracy and the ability to solve the boundary conditions exactly. Another advantage that this method enjoys is the relative computer efficiency with which it performs with respect to total computational time. However, in order to utilize this model to accurately predict the behavior of the motion of a vortex pair in nature, it is necessary that a means be discovered to minimize the impact of the numerical instabilities. Finite Element and Finite Difference techniques were also considered as a means of solving this problem but were determined to be too cumbersome and computationally intensive.

The initial step in the task of minimizing numerical instabilities within this distributed vortex model is to identify which variables most affect the performance of the numerical code. In concert with this task is the requirement to qualitatively assess the relative sensitivity of

the code to each changing variable. Finally, after each variable has been qualitatively optimized, additional methods must be implemented to further improve the numerical stability of the model for lower Froude numbers. The effect of the following parameters were investigated:

δ: desingularization parameter

N: total number of free surface discrete vortices

xmax: maximum x/b_0 position

xv: center of the surface vortex distribution (x/b_0)

Upon the completion of the parametric study, a re-discretization method was devised and implemented.

B. DESINGULARIZATION PARAMETER (δ)

1. Introduction

Leeker [Ref 11] discussed a desingularization method introduced by Rosenhead [Ref 12] which uses a smoothing parameter to remove the singularity at the center of a given vortex and to minimize the induced velocity of a vortex on its nearest neighbors. Utilizing this method of desingularization, equation (3) becomes:

$$\frac{dw}{dt} = u - iv = -\frac{i(z-z_0)^2}{2\pi(z-z_0)\left[(z-z_0)^2+\delta^2\right]} + \frac{i(z+\bar{z}_0)^2}{2\pi(z+\bar{z}_0)\left[(z+\bar{z}_0)^2+\delta^2\right]}$$
$$+\sum_{k=1}^{m}\frac{i\Gamma_m(z-z_1)^2}{2\pi(z-z_1)\left[(z-z_1)^2+\delta^2\right]} - \sum_{k=1}^{m}\frac{i\Gamma_m(z+\bar{z}_1)^2}{2\pi(z+\bar{z}_1)\left[(z+\bar{z}_1)^2+\delta^2\right]} \quad (4)$$

Clearly, this method of desingularization eliminates the unnatural infinite velocity at the vortex center and allows the operator to more closely space individual vortices at the free surface. Reduced inter-vortex spacing minimizes the leakage problem arising from widely spaced vortices, yet without the desingularization parameter, this close spacing would immediately lead to individual surface vortices rotating about one another, creating irreparable numerical instabilities. It is clear that as the spacing between vortex elements is increased, the effect of δ on the performance of the code would diminish accordingly. In order to more fully understand the impact of this de-singularization, a systematic parametric study was undertaken.

From earlier investigations by Elnitsky and Leeker [Refs. 10, 11] the optimum parameters for executing the numerical model and ensuring that it would progress an adequate amount of time were qualitatively determined to be:

Number of surface vortices (N)	76
Froude number (Fr)	.35
Starting depth (d_0)	-3.0
Starting time (T*)	-3.00

2. **Application**

The smoothing parameter δ was varied from 0.05 to 0.15 and the program was executed from a non-dimensional starting time of -3.00. The choice of δ was governed by the number of surface elements that would be affected at one time by a given vortex. If δ is chosen too large with respect to the quantity $(z-z_i)$, the program will

essentially ignore several consecutive vortex contributions in its calculation of the velocity field; this is particularly prevalent at the early stages of the motion where the vortex spacing is comparatively small near the axis of symmetry. Ideally, the goal was to avoid having δ mask more than two consecutive surface vortices at the beginning of the distribution and yet purposely mask vortices where the numerical instabilities form. This allows the calculation to proceed with each vortex having only a minor effect on its nearest neighbors but still having the full effect on more distant vortices. As a result, the operator may space vortices very close together and yet still minimize the instabilities which would otherwise occur.

Table 1 summarizes a representative number of executions of the numerical model while holding all other variables constant and varying δ from .05 to .15. The breakdown time represents the last reliable time ($\pm$ five time steps) where the free surface is not unnaturally formed. As can be seen clearly from Figure 1, the lowest value of δ (.05) is unacceptable. The free surface deforms in an entirely unnatural fashion at all non-dimensional times later than -1.4. Run 2 demonstrates significant improvement with only a very minor increase in δ (Figure 2). For subsequent runs with a slightly increasing δ value, the gain in extended execution time is minimized and appears to converge somewhat to a non-dimensional time of about -1.0. Figures 3 through 7 illustrate the form of the free surface for each run at the last reliable time just prior to the halt of the execution due to numerical

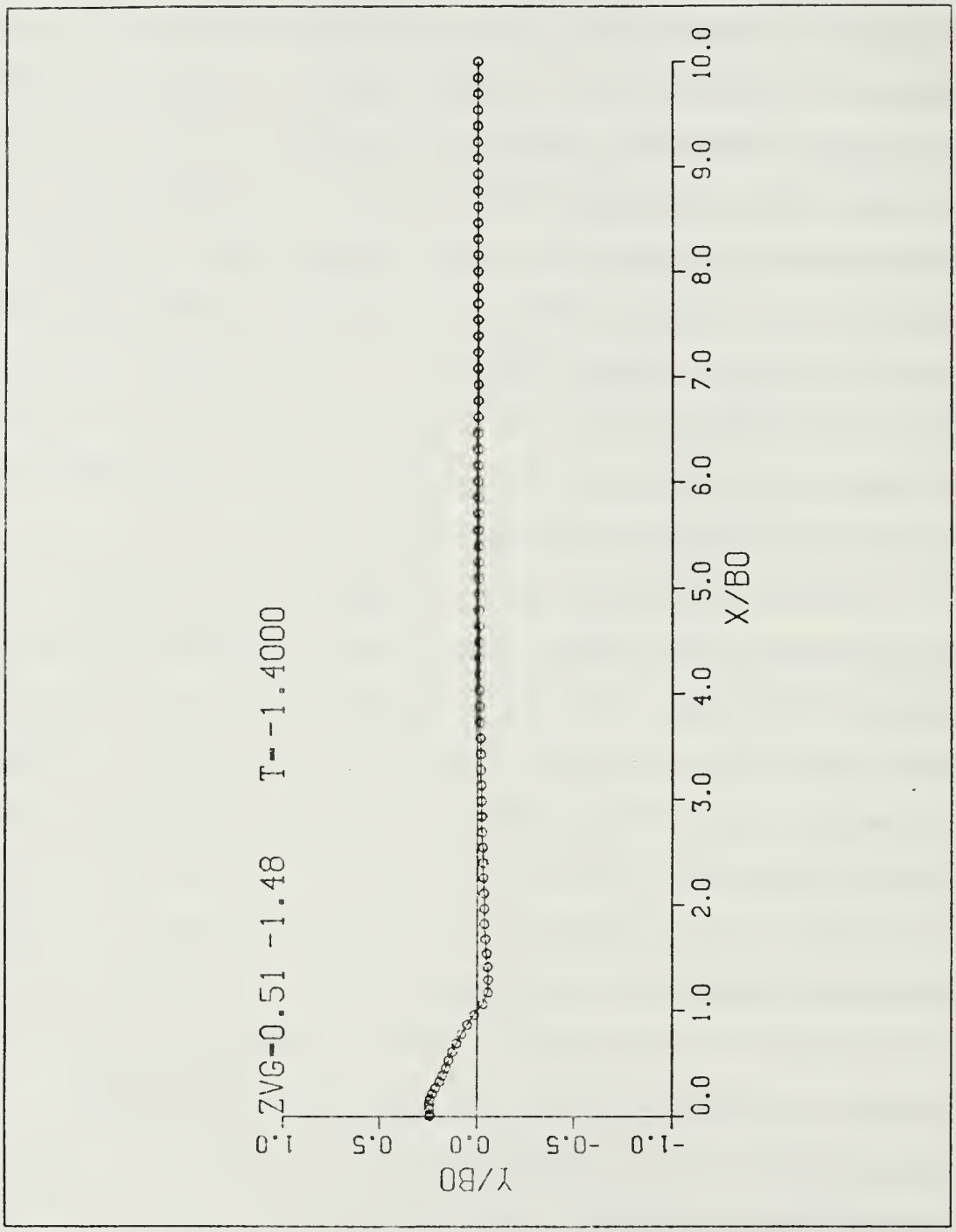

Figure 1. **Run 1, Free Surface Deformation, δ = .05, T* = –1.4**

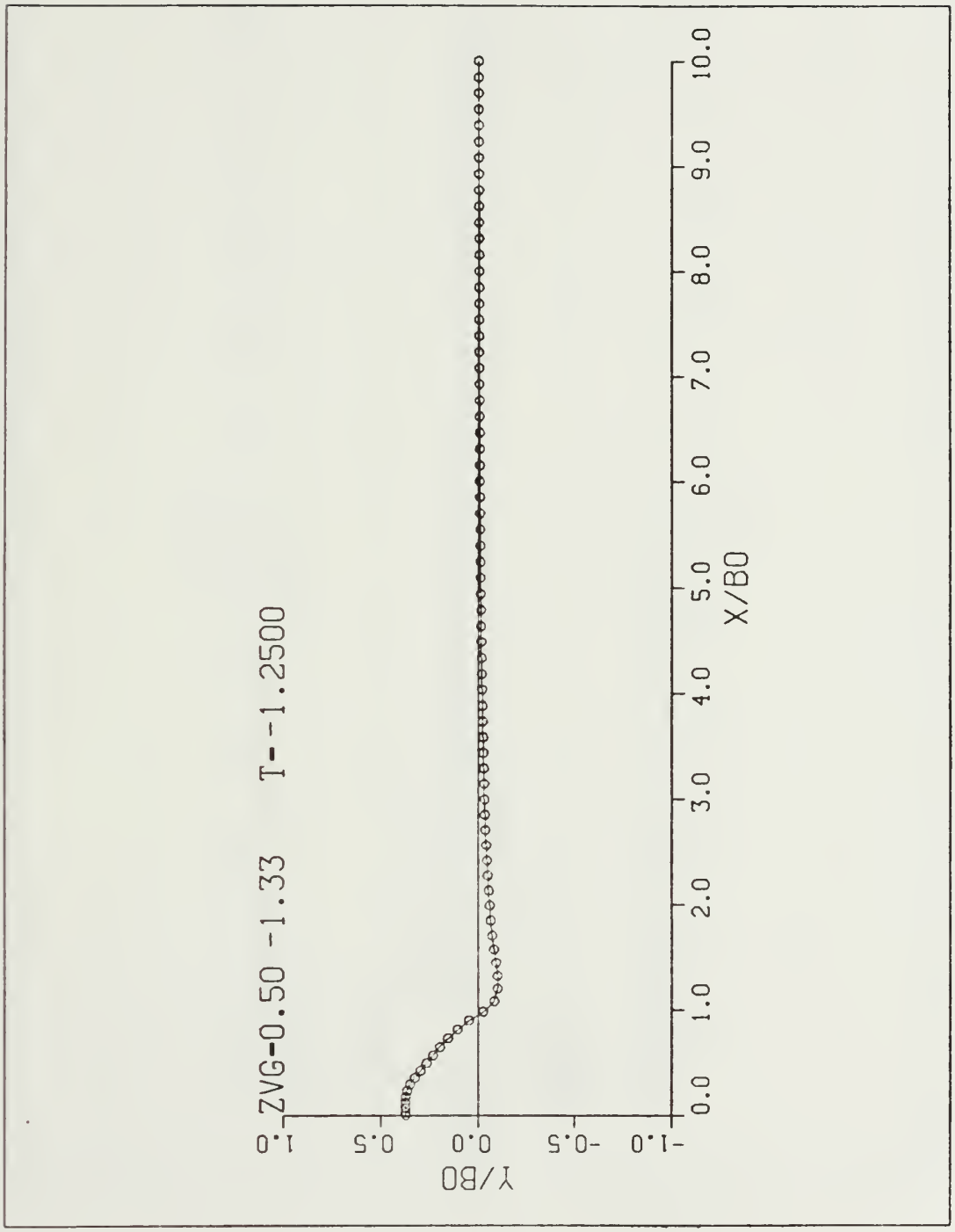

Figure 2. **Run 2, Free Surface Deformation, δ = .07, T* = –1.25**

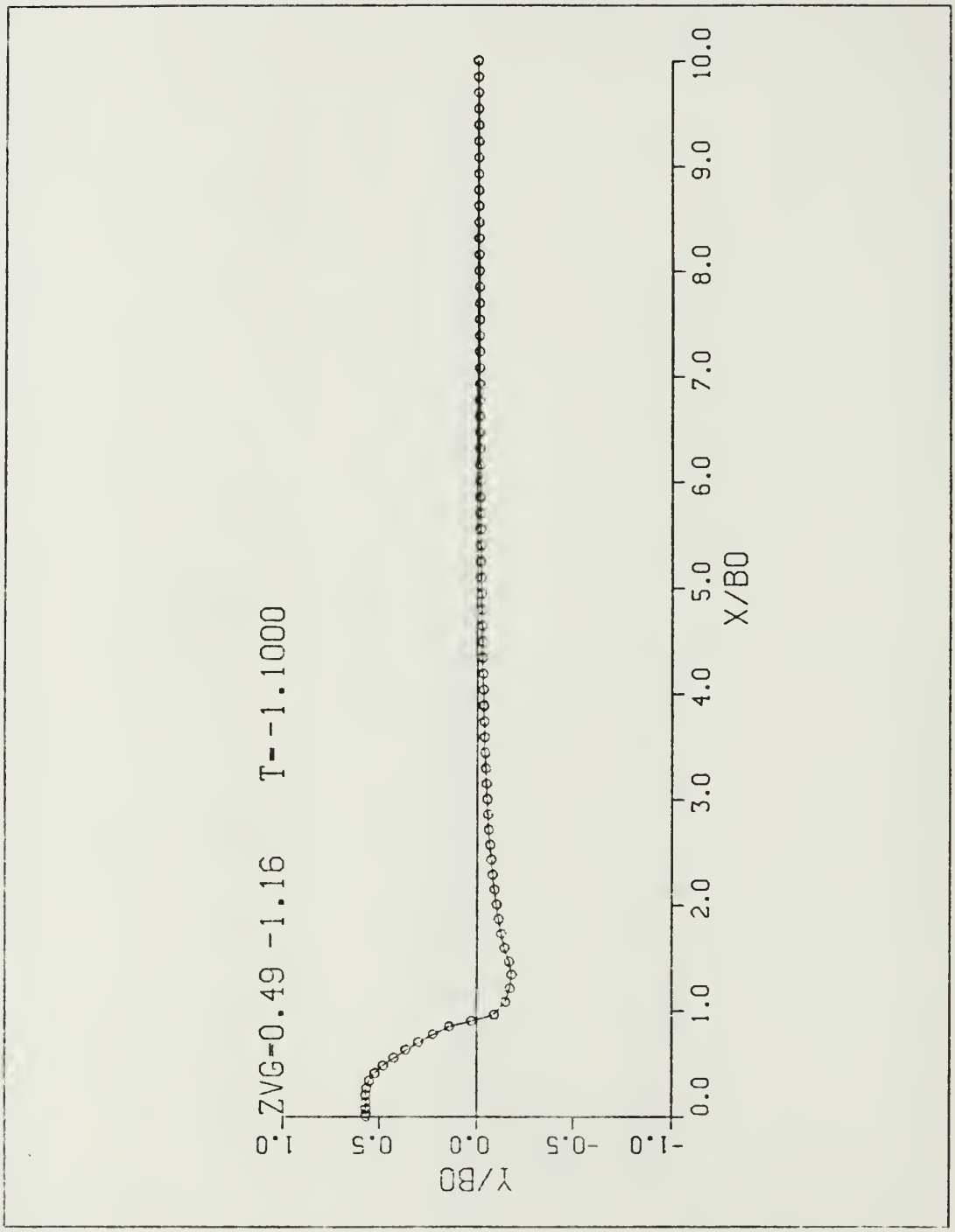

Figure 3. **Run 3, Free Surface Deformation, δ = .09, T* = -1.1**

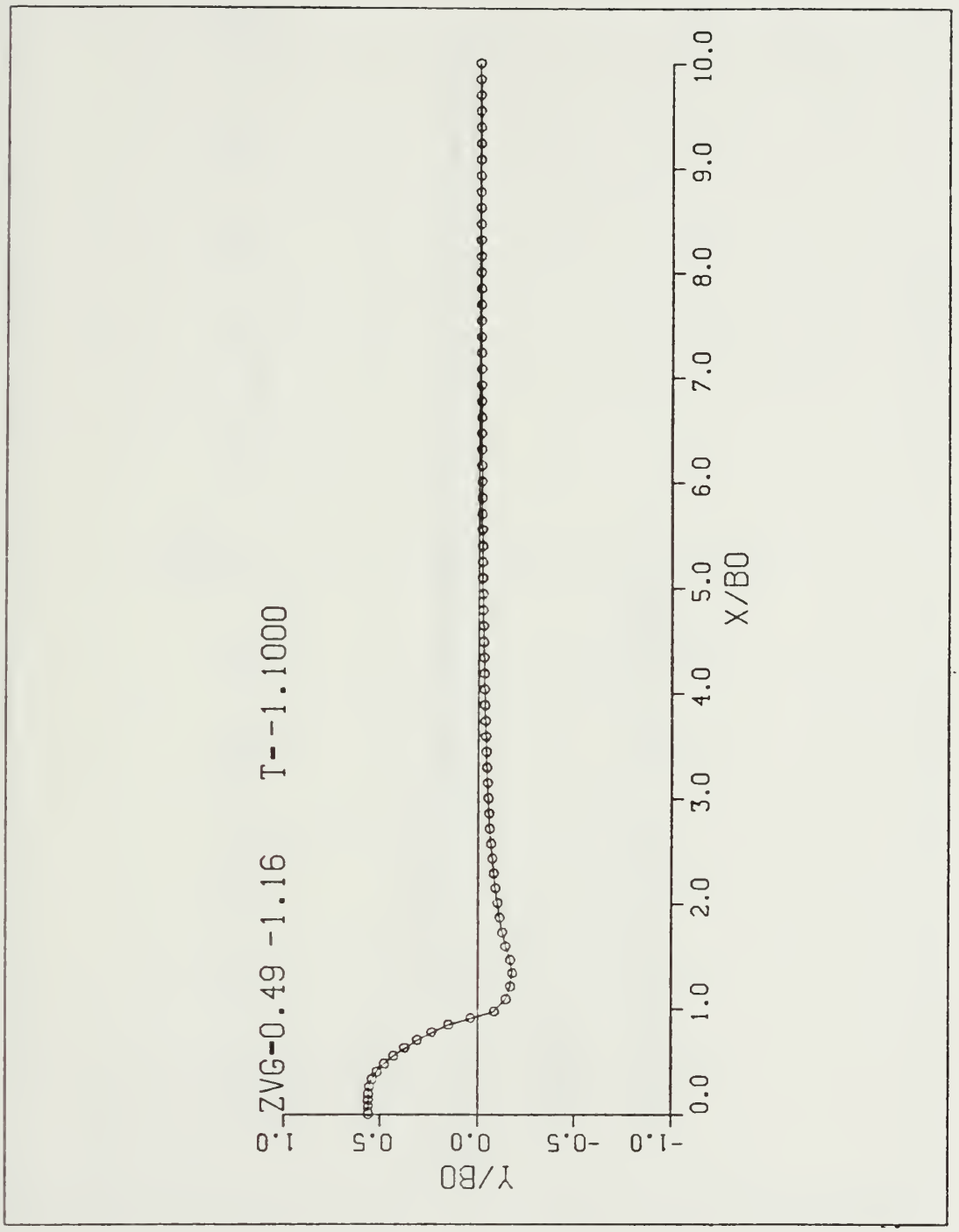

Figure 4. **Run 4, Free Surface Deformation, δ = 0.1, T* = -1.1**

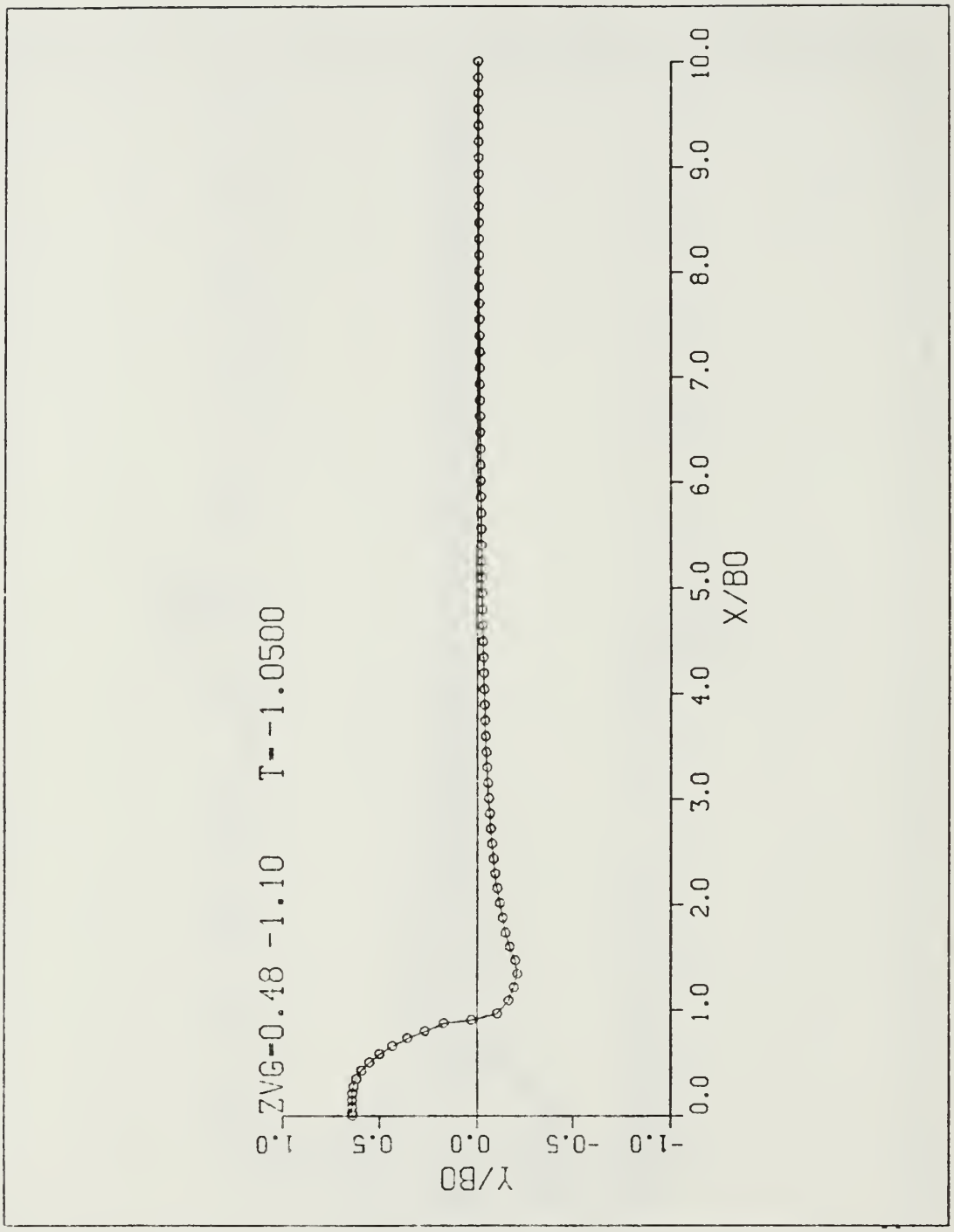

Figure 5. **Run 5, Free Surface Deformation, δ = .11, T* = -1.05**

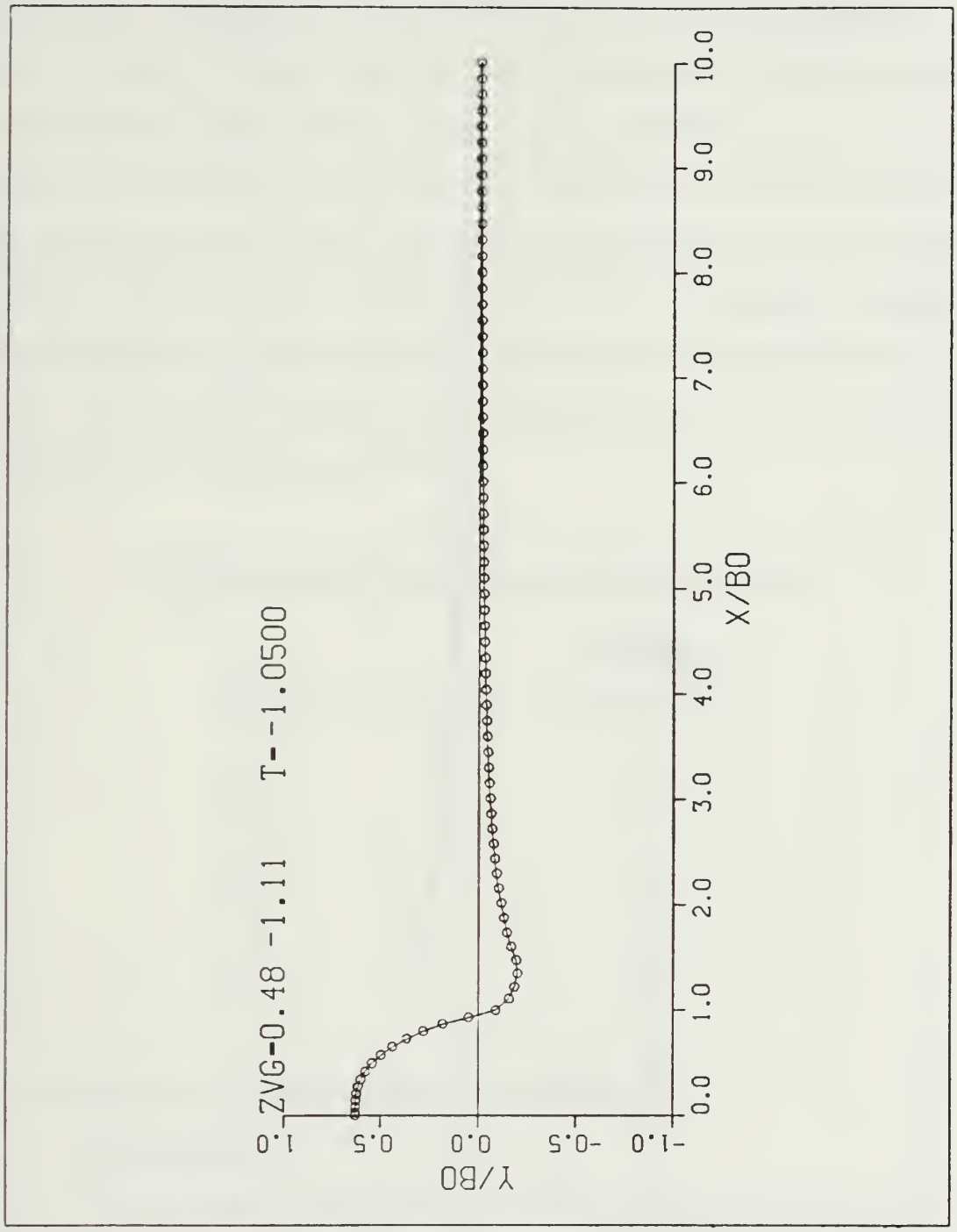

Figure 6. **Run 6, Free Surface Deformation, δ = .13, T* = –1.05**

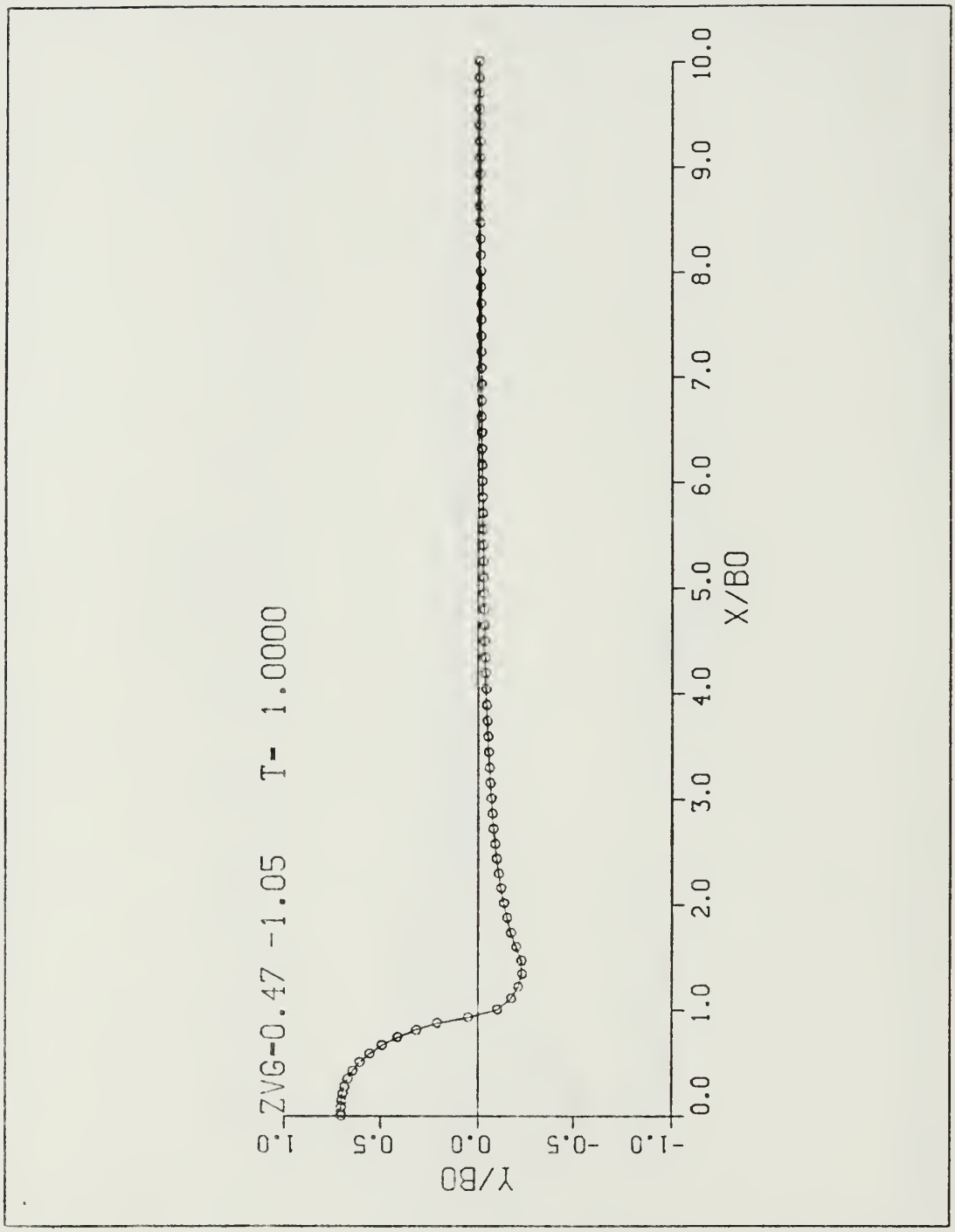

Figure 7. **Run 7, Free Surface Deformation, δ = .15, T* = –1.0**

instabilities. Essentially, any increase in δ above approximately 0.1 serves no other purpose than to mask a number of surface vortices unnecessarily, with only a trivial gain in additional time steps of execution. Figures 8 through 14 represent the free-surface deformation at execution-halt time and clearly demonstrate that the gain in program execution time is minimal. The numerical model is surprisingly insensitive to this parameter once it has accomplished its purpose of removing the singularity. The qualitatively chosen optimum value of δ was determined to be 0.1.

TABLE 1

VARIATION OF δ VERSUS BREAKDOWN TIME

Run #	δ	Breakdown Time (T*)
1	.05	-1.4
2	.07	-1.25
3	.09	-1.1
4	.1	-1.1
5	.11	-1.05
6	.13	-1.05
7	.15	-1.0

C. NUMBER OF FREE SURFACE VORTICES (N)

1. Introduction

The number of free surface vortices present during any particular run is automatically calculated by a subroutine within the

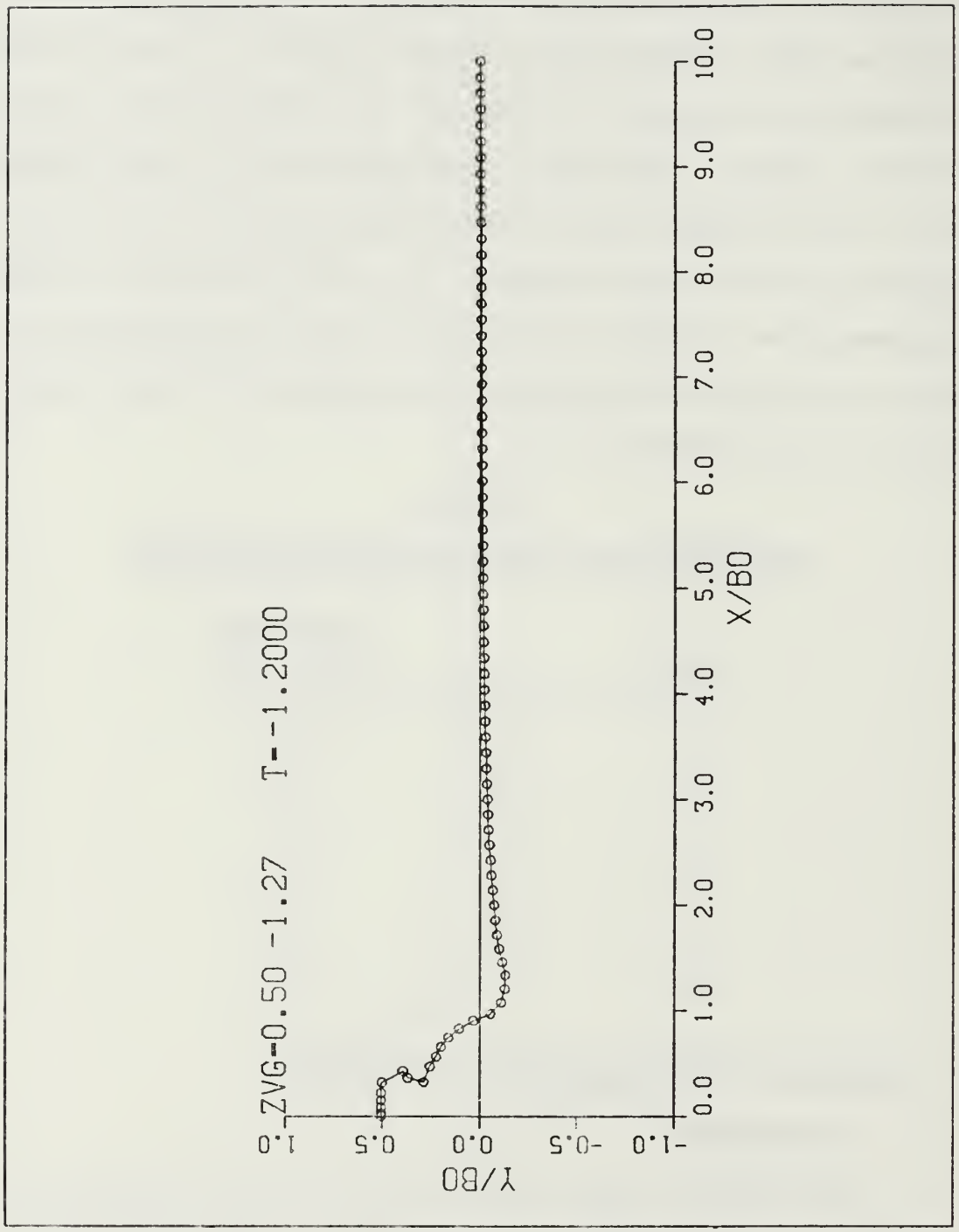

Figure 8. **Run 1, Free Surface Deformation, δ = .05, Execution Halt T*=–1.20**

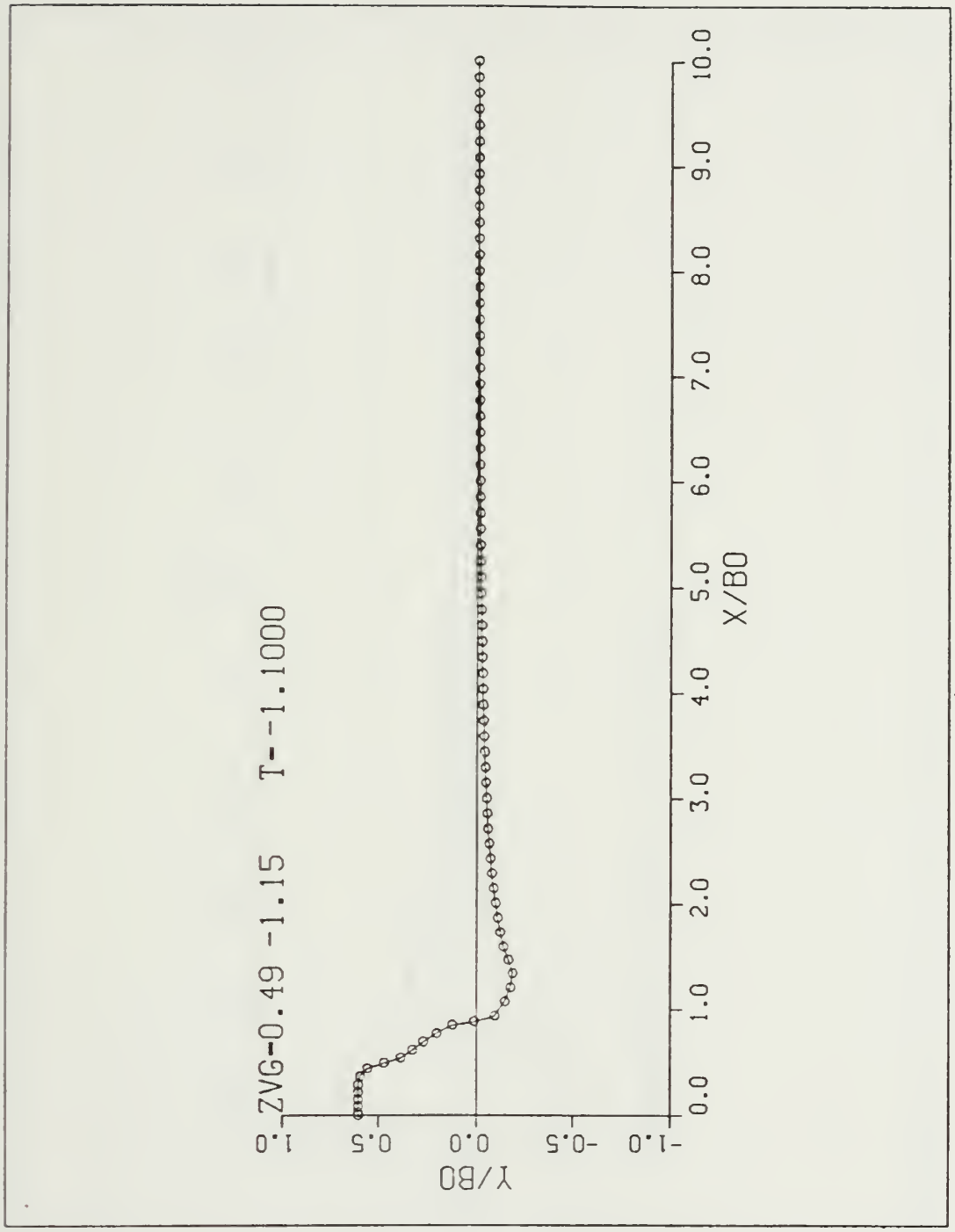

Figure 9. **Run 2, Free Surface Deformation, δ = .07, Execution Halt T* = –1.10**

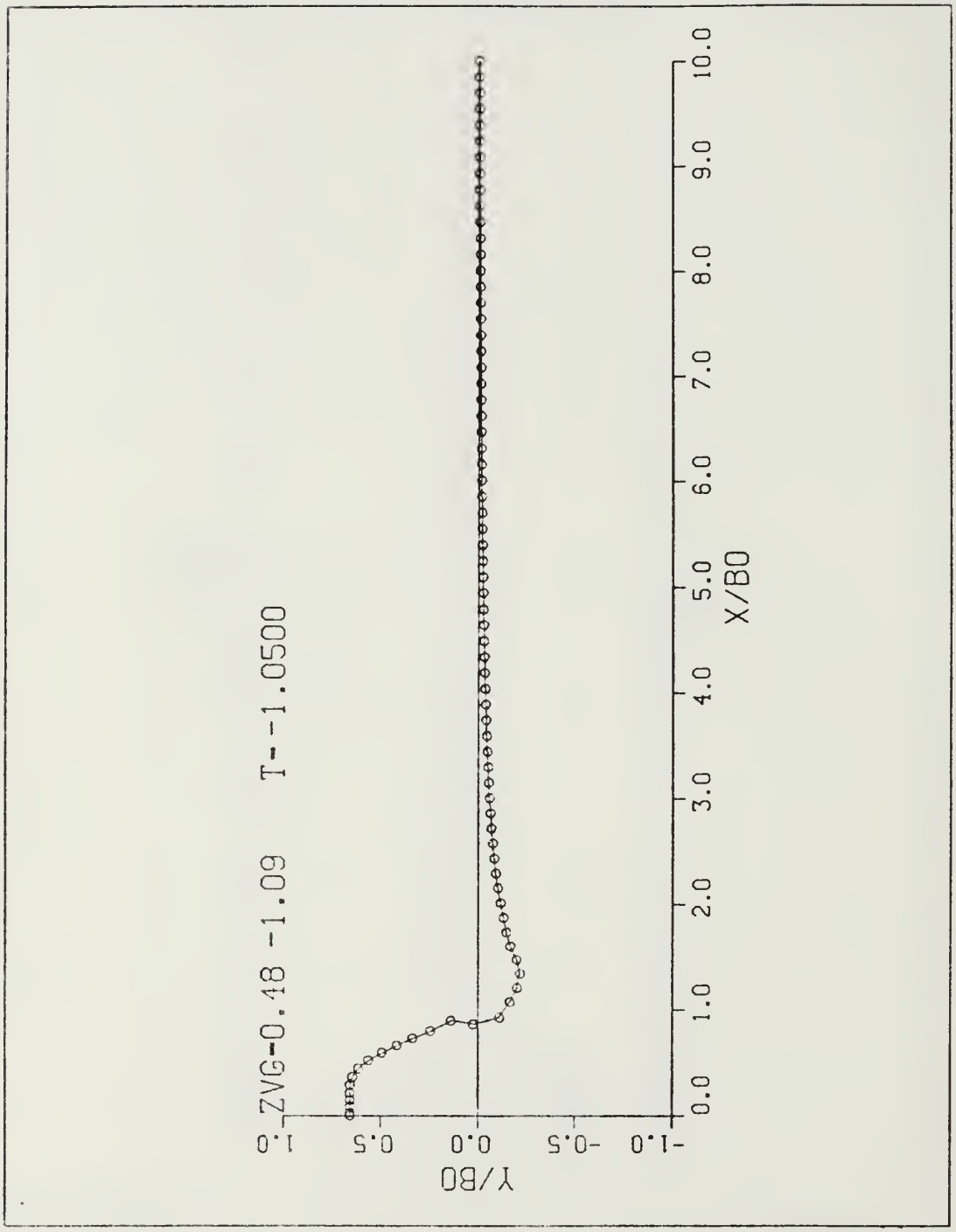

Figure 10. **Run 3, Free Surface Deformation, δ = .09, Execution Halt T* = –1.05**

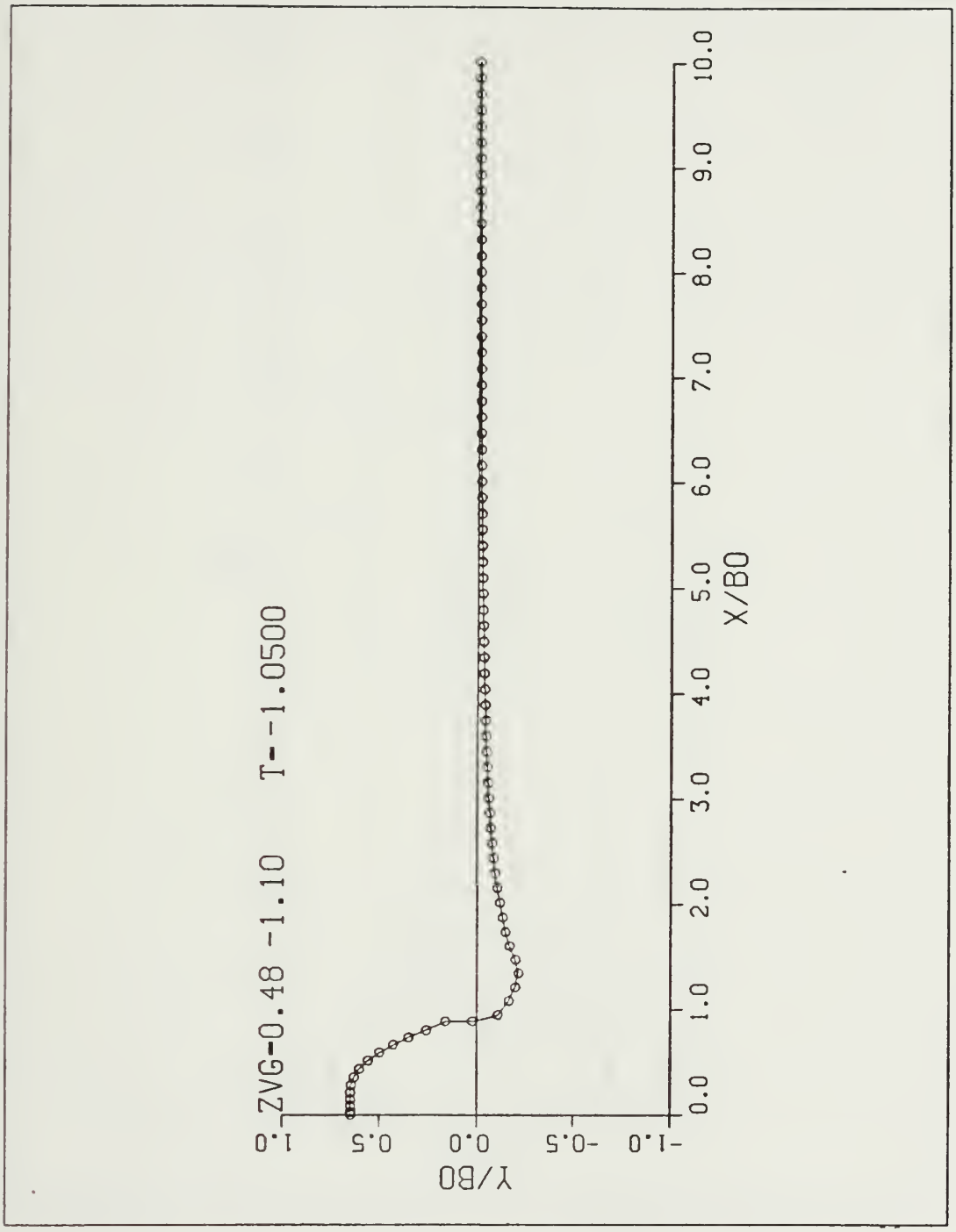

Figure 11. **Run 4, Free Surface Deformation, δ = .10, Execution Halt T* = –1.00**

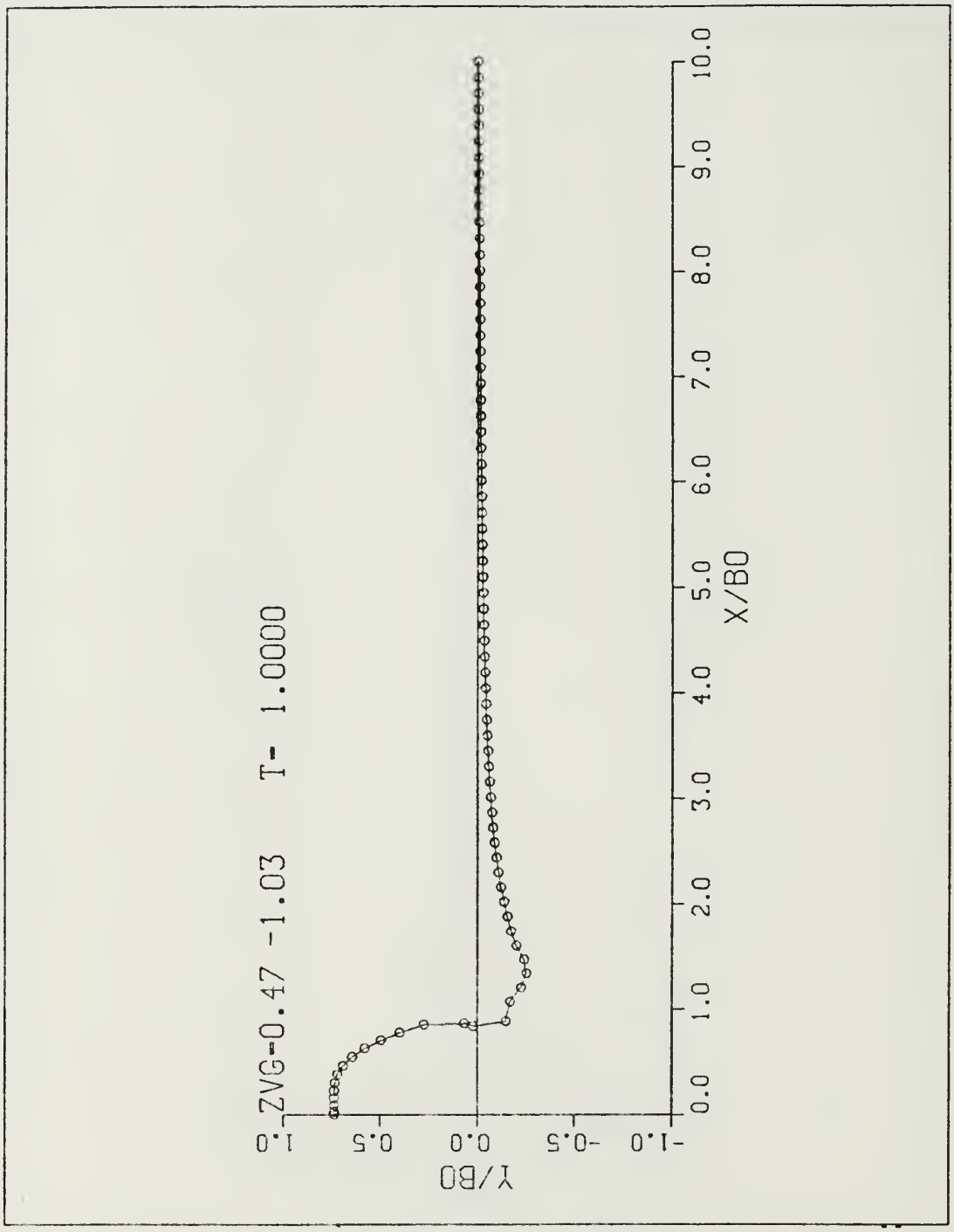

Figure 12. **Run 5, Free Surface Deformation, δ = .11, Execution Halt T* = –1.00**

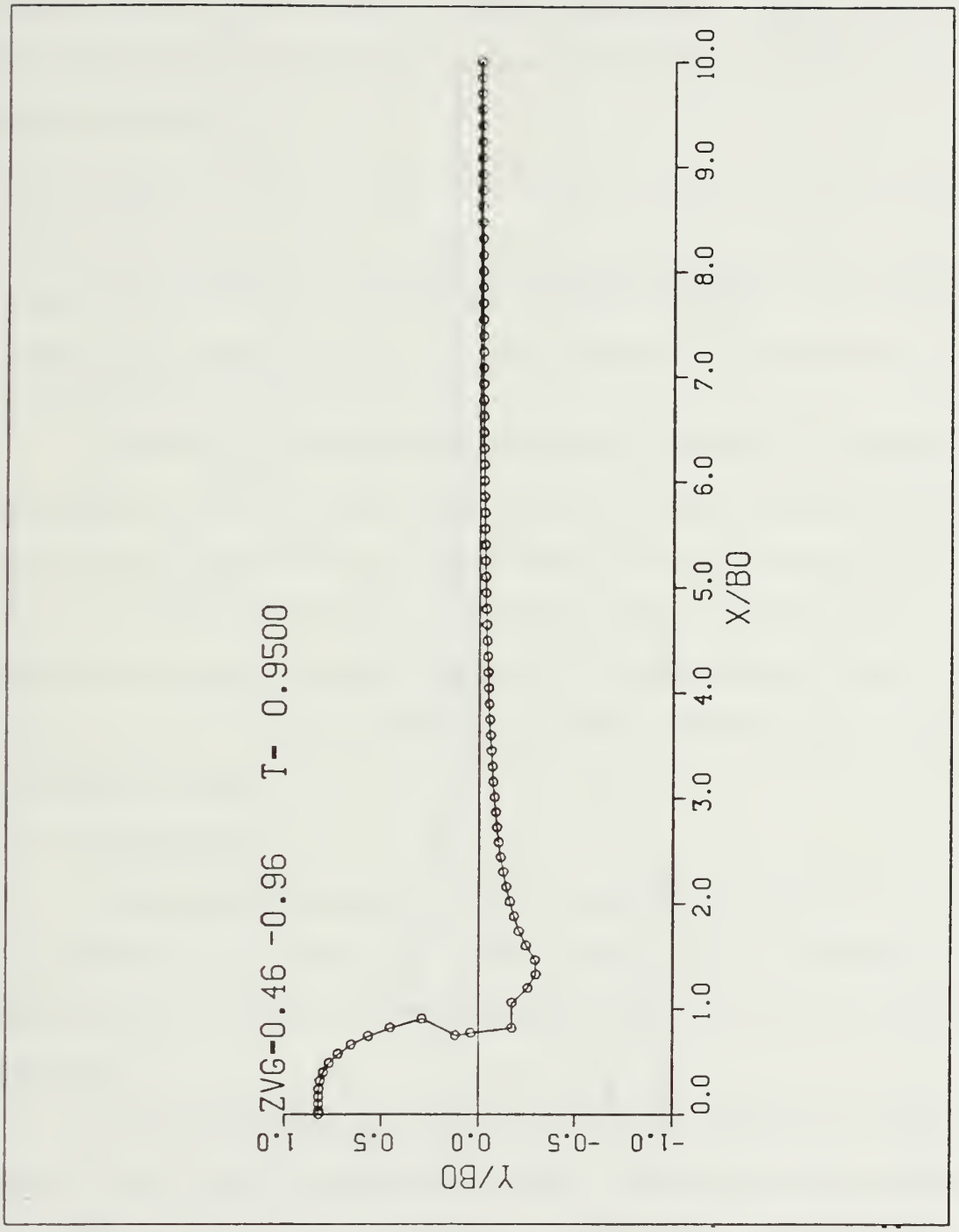

Figure 13. **Run 6, Free Surface Deformation, δ = .13, Execution Halt T* = –0.95**

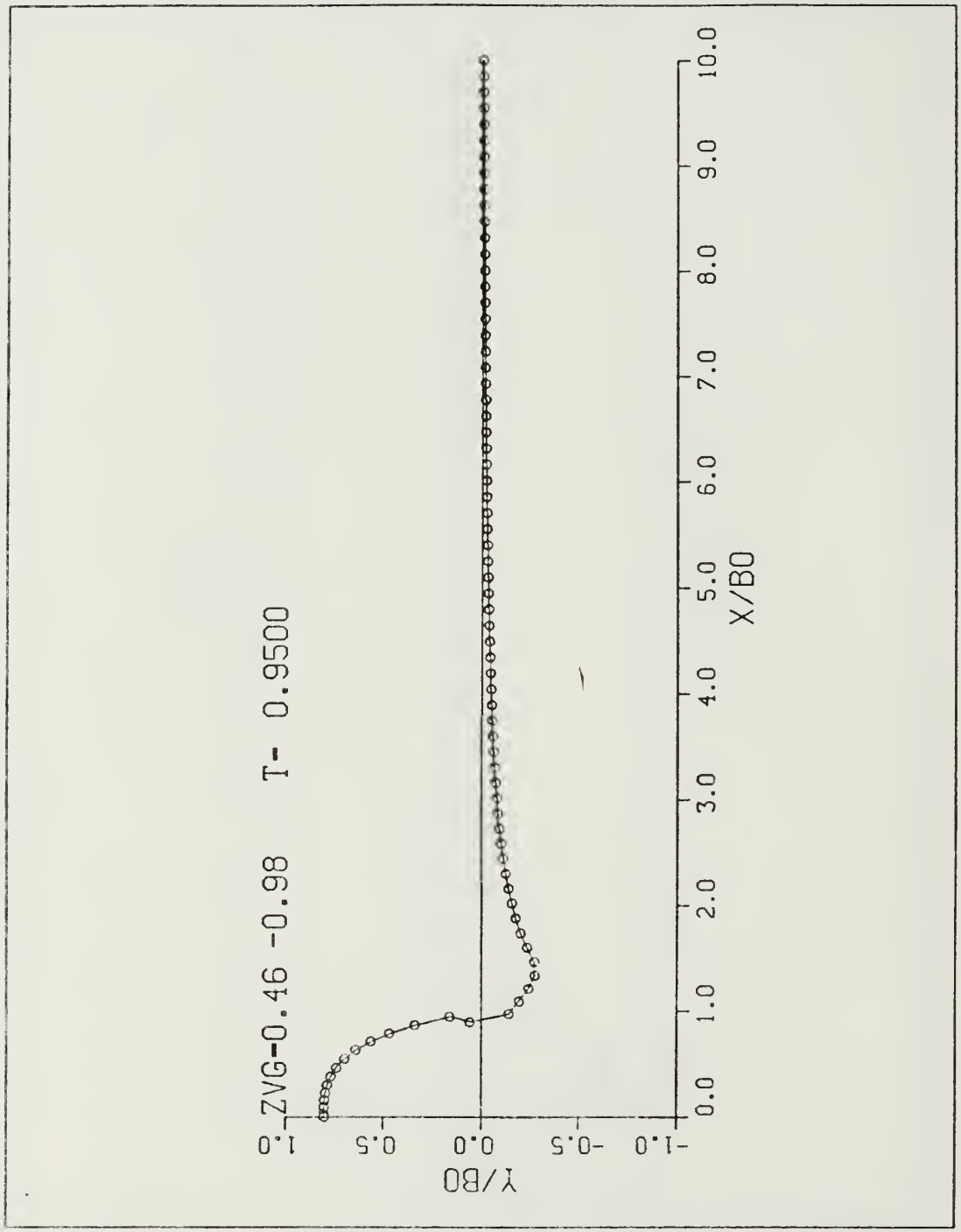

Figure 14. **Run 7, Free Surface Deformation, δ = .15, Execution Halt T* = –0.95**

program when given certain desired parameters. The operator directs the program to place the surface vortices after deciding on the following conditions:

a. The initial distance between the first free surface vortex and the centerline.

b. The position (x/b_0) where the geometric progressional placement of vortices ends and constant spacing begins.

c. The actual distance (x/b_0) between vortices after the point in (b) above has been reached.

The details of the calculation of vortex spacing is not particularly important but the actual decision of how many vortices to place along the free surface will critically affect the performance of the model. As discussed earlier, as vortex density increases, although leakage decreases (a desirable result), the velocity impact of one vortex upon another increases and rapidly forces the breakdown of the model prematurely.

2. Application

Numerous program executions were completed to determine the sensitivity of the numerical model to the number of discrete free surface vortices. Table 2 represents the results of a portion of these executions.

The desingularization parameter (δ) was adjusted in order to maintain the criteria established earlier (avoid masking vortices unnecessarily yet still "cover" the breakdown point). This adjustment of δ was necessary to ensure that the model remained as close to its natural form as possible. For example, if δ was maintained at 0.1

during run #10, it would effectively mask a much larger number of discrete vortices and thus introduce an unnecessary artificiality into the execution of the model. Similarly, if δ was maintained at 0.1 during run #8, the singularity in the velocity expression would barely even be removed. Figures 15 through 17 depict the formation of the free surface immediately before breakdown.

TABLE 2

VARIATION OF N VERSUS BREAKDOWN TIME

Run	δ	N	Breakdown Time (T*)
8	0.18	38	-1.0
9	0.10	76	-1.1
10	0.085	149	-1.1

The results of these executions reveal the model's insensitivity to a variable number of discrete free surface vortices. The only concern remaining to the operator as a result of this particular study is to balance the leakage versus the propensity of the vortices to orbit about each other, as discussed earlier, and to consider the total computational time required to complete each run. For example, Runs #8 and #9 require only a moderate amount of time to complete, but Run #10 required over 90 minutes of real-time computation. As a result, any execution with $N \geq 149$ must be executed during low-computer-use time only. Qualitatively weighing these factors, it was determined

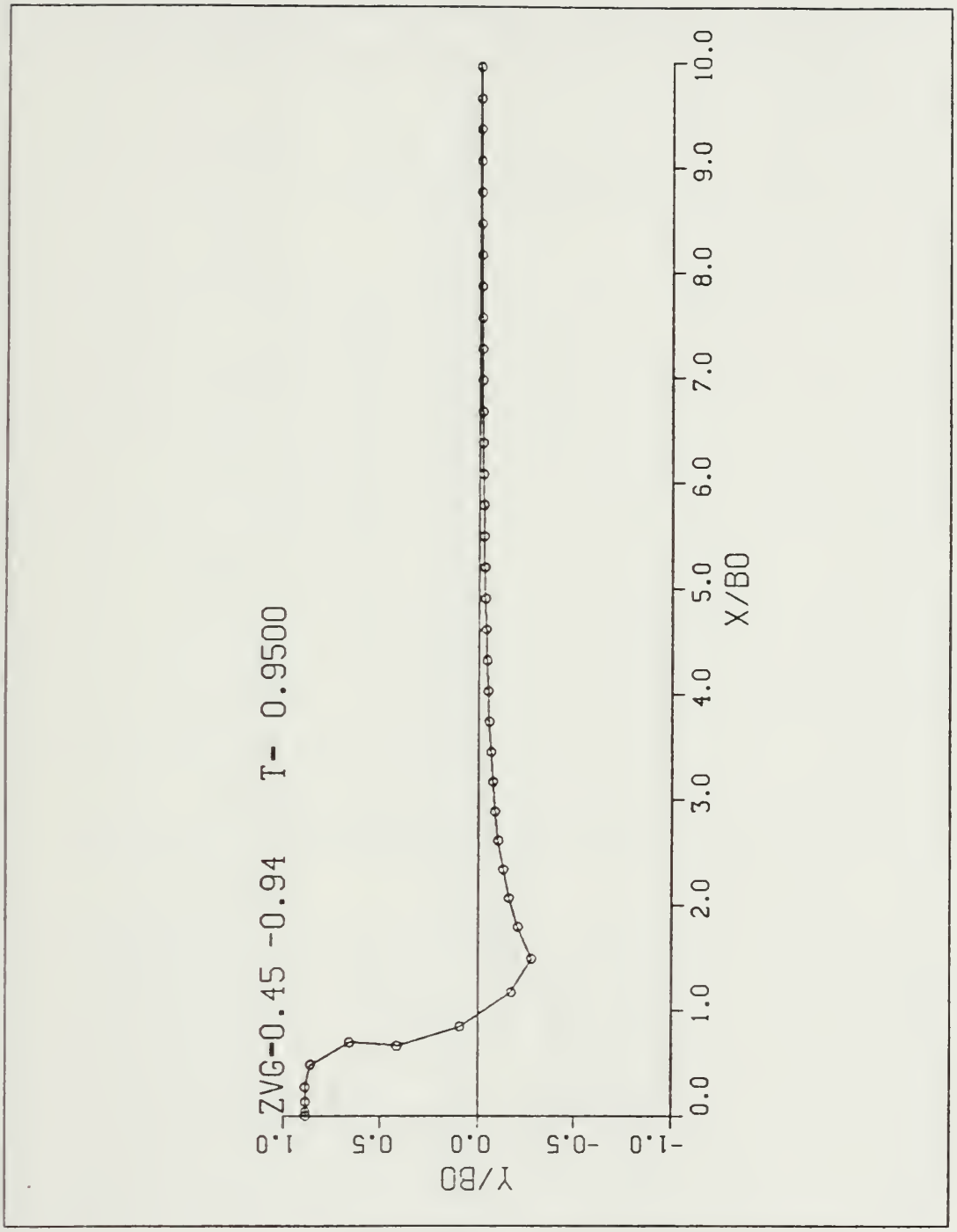

Figure 15. **Run 8 , Free Surface Deformation, N = 38**

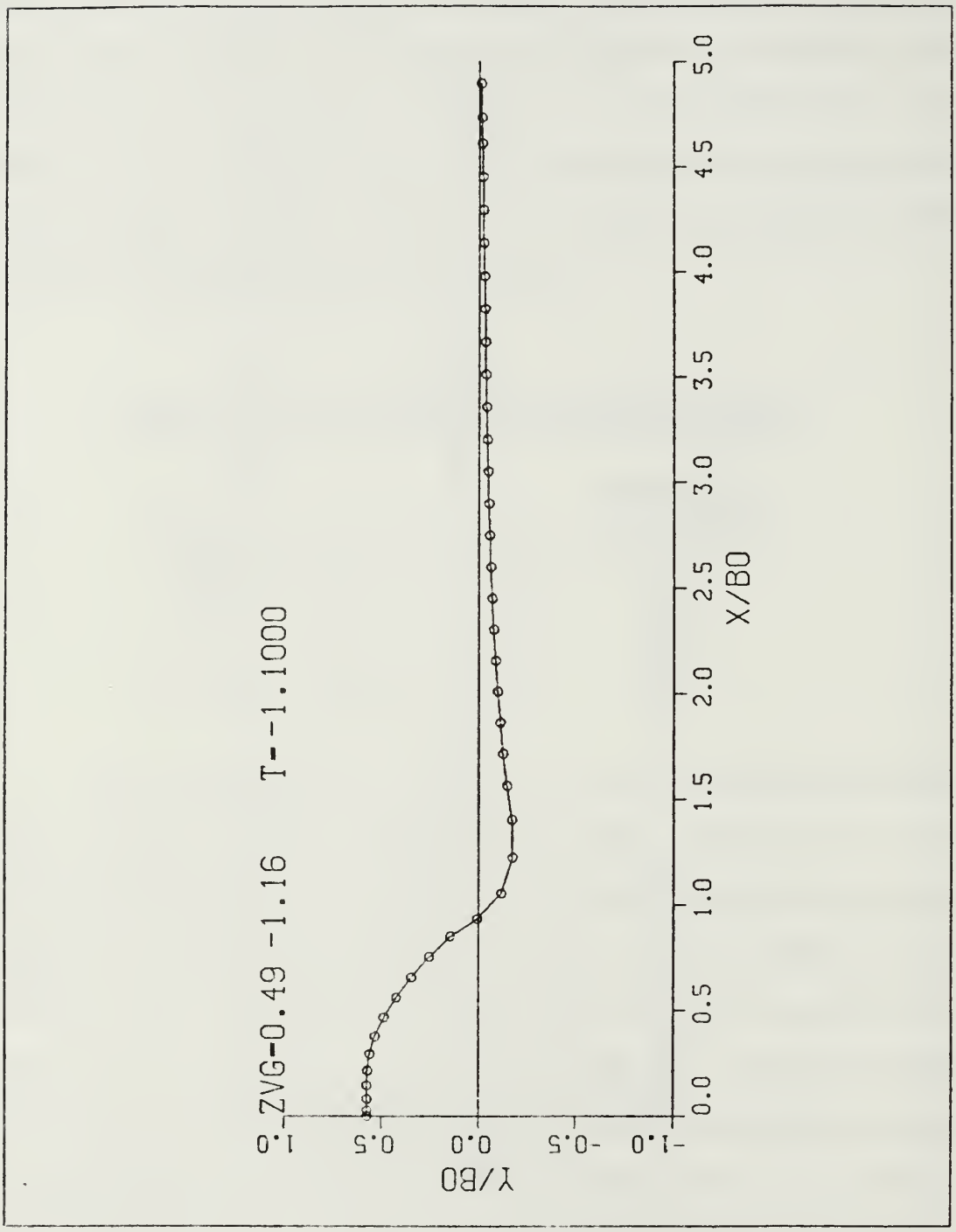

Figure 16. **Run 9, Free Surface Deformation, N = 76**

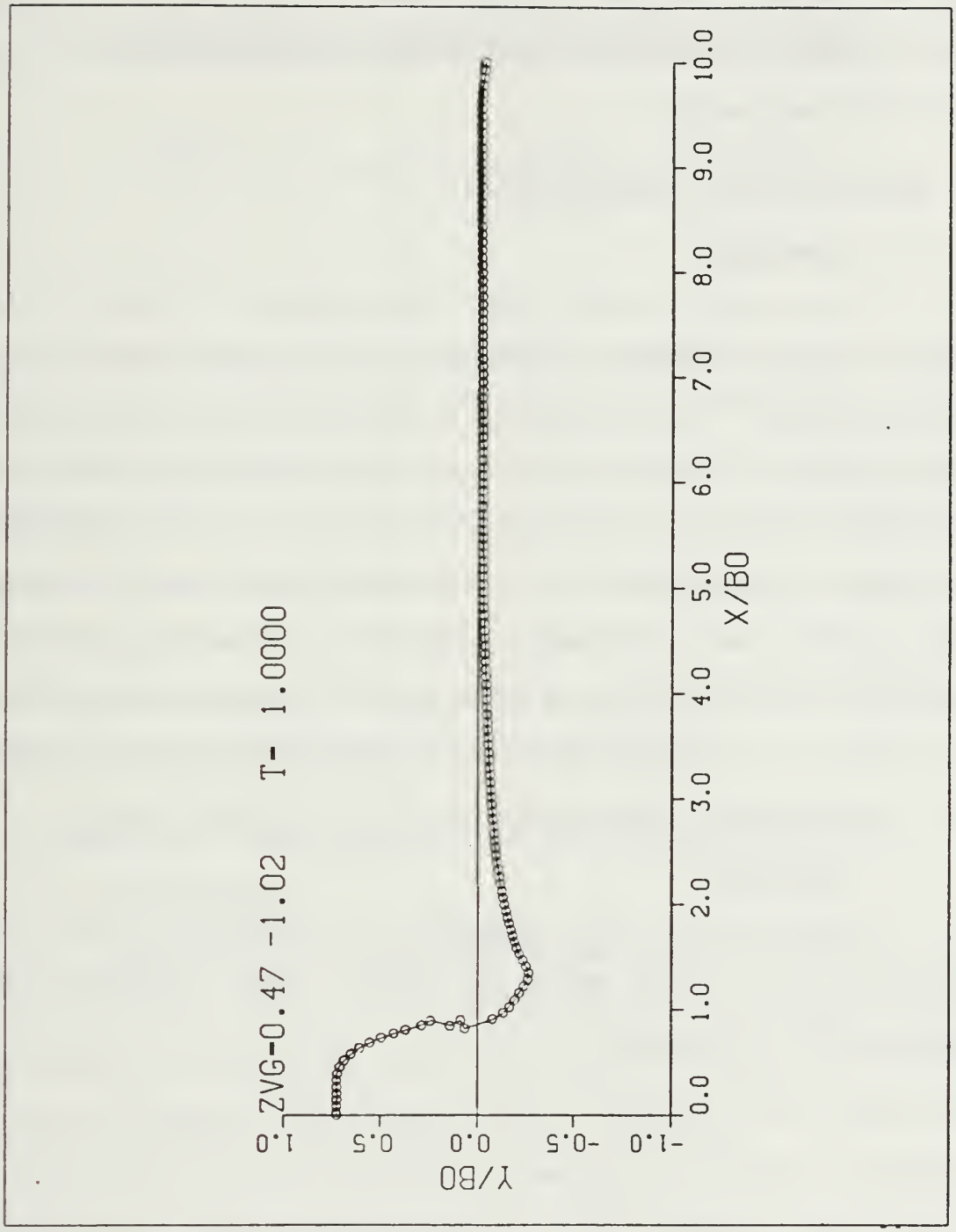

Figure 17. **Run 10, Free Surface Deformation, N = 149**

that the optimum number of free surface vortices was 76. Average vortex density (N/xmax) was held constant throughout the remainder of the parametric study.

D. MAXIMUM X/B_0 VALUE (XMAX)

1. Introduction

Very closely related to the total number of vortices in the model is the total length of free surface that they will be responsible for representing. It is not desirable to have the vortices represent an extensive stretch of free surface since it would prolong the total computation time and serve no meaningful function. It is also undesirable to restrict the extent of the free surface so severely that it would not truly represent nature as closely as possible. The simple goal of the study of the numerical model's sensitivity to a changing xmax value is to confirm the theory that the model would behave similarly at different N, provided the vortex density remained relatively constant.

2. Application

Two executions were completed in an attempt to confirm the theory of vortex density within the model. Table 3 represents the results of these executions.

TABLE 3

VARIATION OF XMAX VERSUS BREAKDOWN TIME

Run #	δ	N	xmax	Breakdown Time (T*)
11	.1	76	10	−1.0
12	.1	38	5	−1.1

From Figures 18 and 19, the form of the free surface demonstrated no significant change when xmax was decreased from 10 x/b_0 to 5 x/b_0. Essentially, there is no major advantage in using a value exceeding about 5 x/b_0 since all vortex action occurs well within that value. The only remaining advantage of varying this parameter is to increase or decrease real CPU time. Obviously, as the value of xmax increases, computational time increases as well. For the remainder of this parametric study, a value of 5 x/b_0 was utilized.

E. CENTER OF THE SURFACE VORTEX DISTRIBUTION (XV)

1. Introduction

Elnitsky [Ref. 10] pointed out that a major advantage of the Boundary Integral method is the propensity of the free surface vortices to migrate to the regions where the radius of curvature of the free surface is smallest. The surface vortices "roll down" the hump of the deformed free surface and collect in the region of the scar. Thus one achieves the greatest discretization at the positions along the free surface where it is most needed.

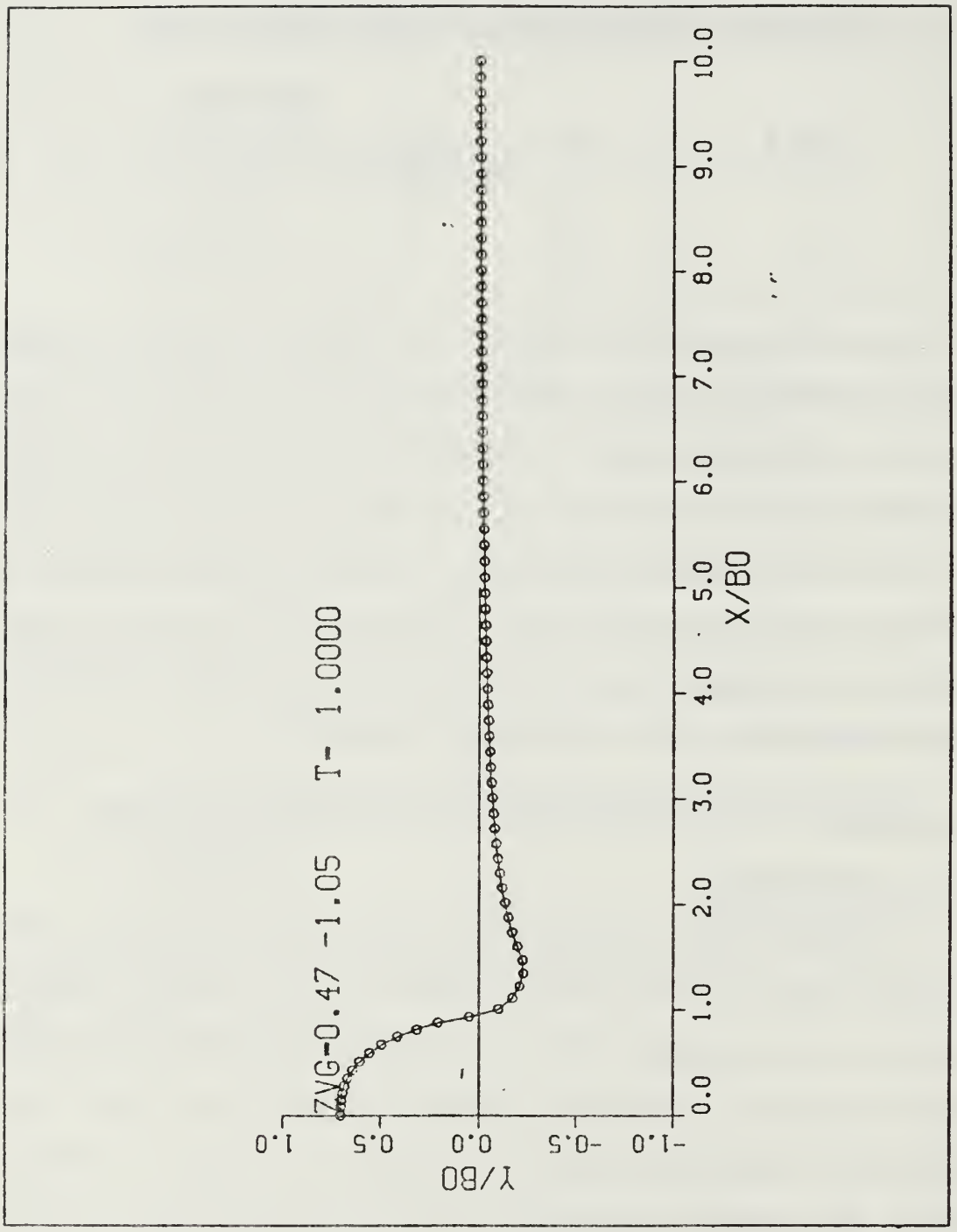

Figure 18. **Run 11, Free Surface Deformation, xmax = 10**

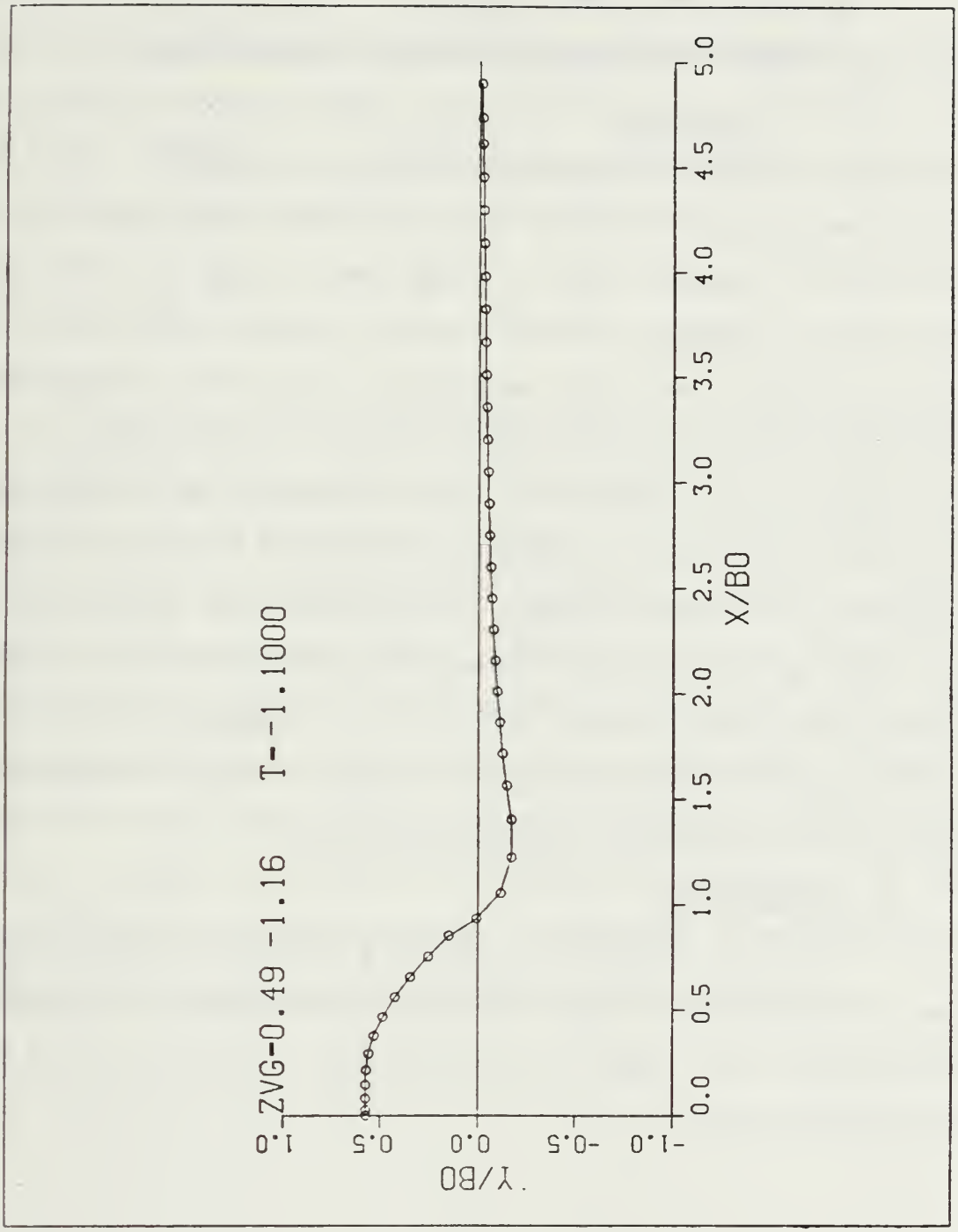

Figure 19. **Run 12, Free Surface Deformation, xmax = 5**

As discussed earlier, the center of free surface vortex distribution is an operator-selected parameter. The algorithm that calculates the initial position of each free surface vortex will allow the distribution of vortices to emanate from any x/b_0 position. From that selected position, a subroutine will geometrically place vortices to the left until the centerline ($x/b_0 = 0$) has been reached and to the right until the x/b_0 position of xmax has been reached. Since the vortex density along the free surface is greatest at the center of distribution, by moving this point the operator can affect the vortex density at any point along the free surface later in time. Naturally, as one progresses away from the center of distribution, this effect is minimized and is eventually eliminated completely. The purpose of the variation of this parameter is to ascertain whether there is an ideal (xv) position enabling the surface vortices to "roll" into an optimum position at the correct time and minimize or delay the onset of the numerical instabilities that are introduced into the free surface.

2. Application

Runs 13 through 15 represent a sample of the executions of the code completed in order to identify the sensitivity of the model to the parameter (xv). Table 4 lists the details of each run and its effect on completion time.

TABLE 4

VARIATION OF xv VERSUS BREAKDOWN TIME

Run #	xv (x/b_0)	Breakdown Time (T^*)
13	1.0	-1.10
14	0.8	-1.05
15	0.5	-1.25

Although the breakdown time of runs 13 through 15 did not vary significantly from earlier runs, the variation of xv resulted in totally unacceptable free surface formations. From Figures 20 through 22, it is noticed that the flat shape of the hump later in time is caused by the relatively low vortex density Also noted is the fact that the free surface vortices continue to "roll downhill" but terminate farther than in previous executions. In fact, this tendency of the surface vortices to roll farther away from centerline actually contributes to the formation of the numerical instabilities by creating sharp corners and large spaces between individual vortices. Accordingly, it was decided to maintain the center of vortex distribution at the centerline.

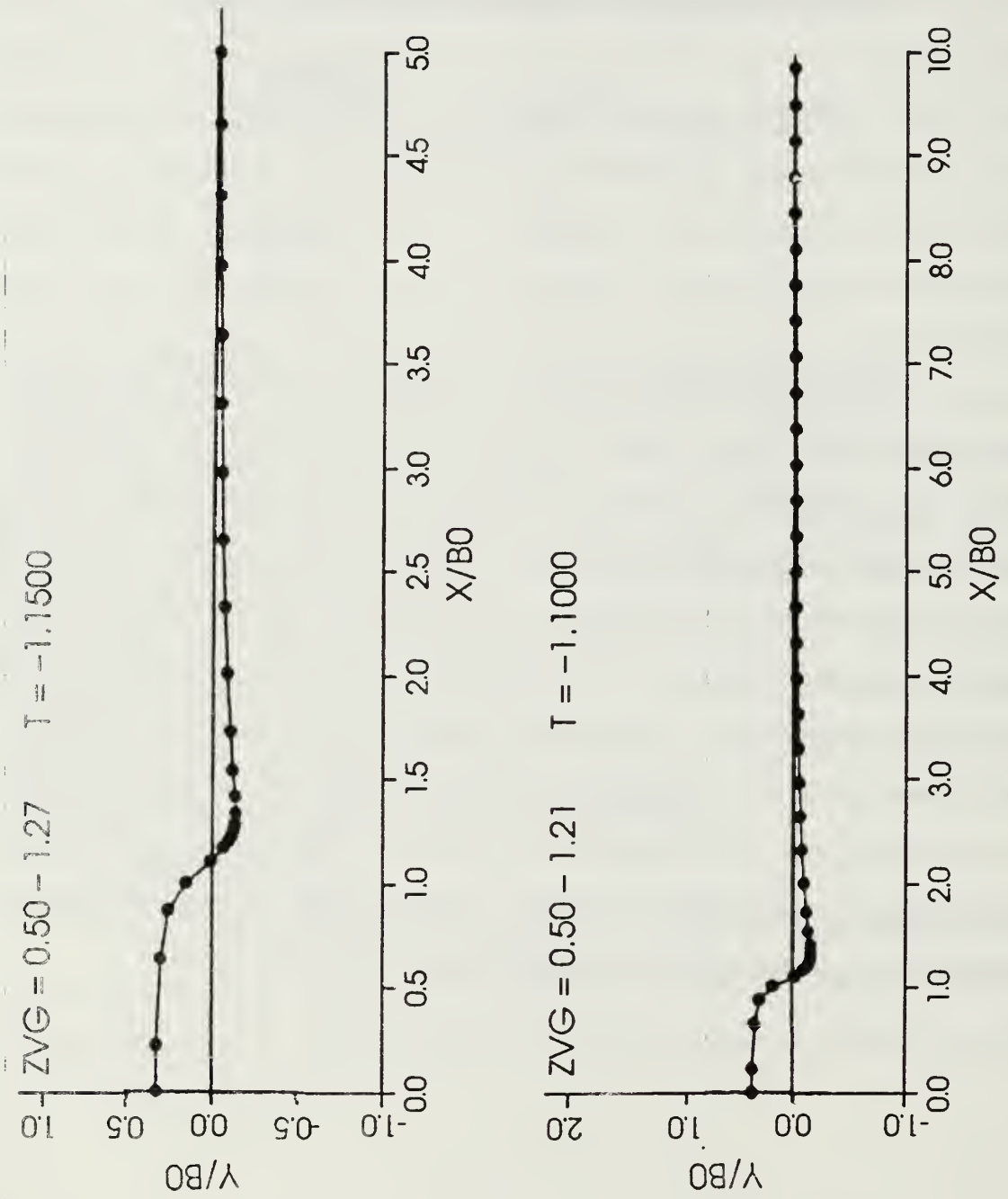

Figure 20. **Run 13, Free Surface Deformation, xv = 1.0**

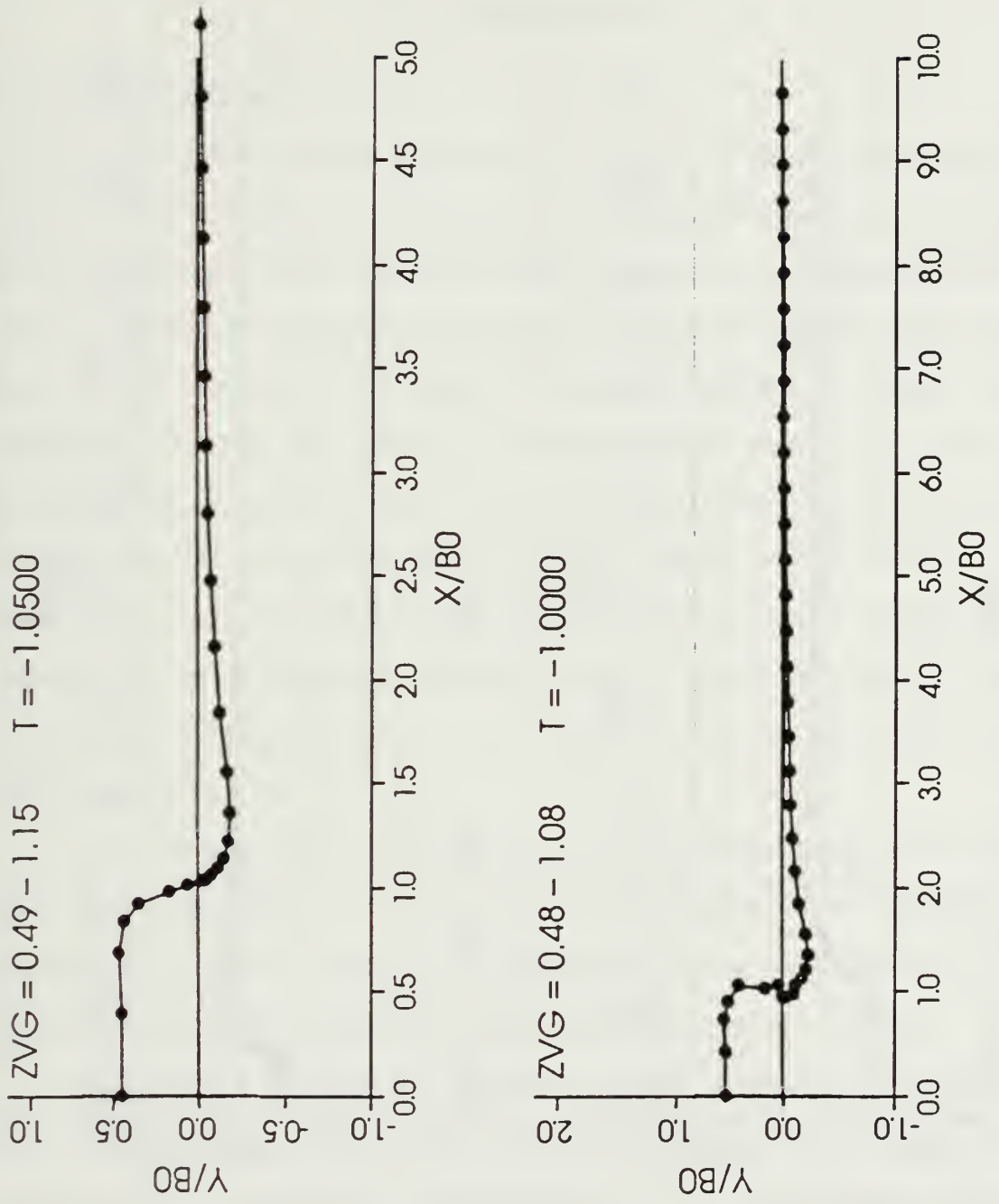

Figure 21. **Run 14, Free Surface Deformation, xv = 0.8**

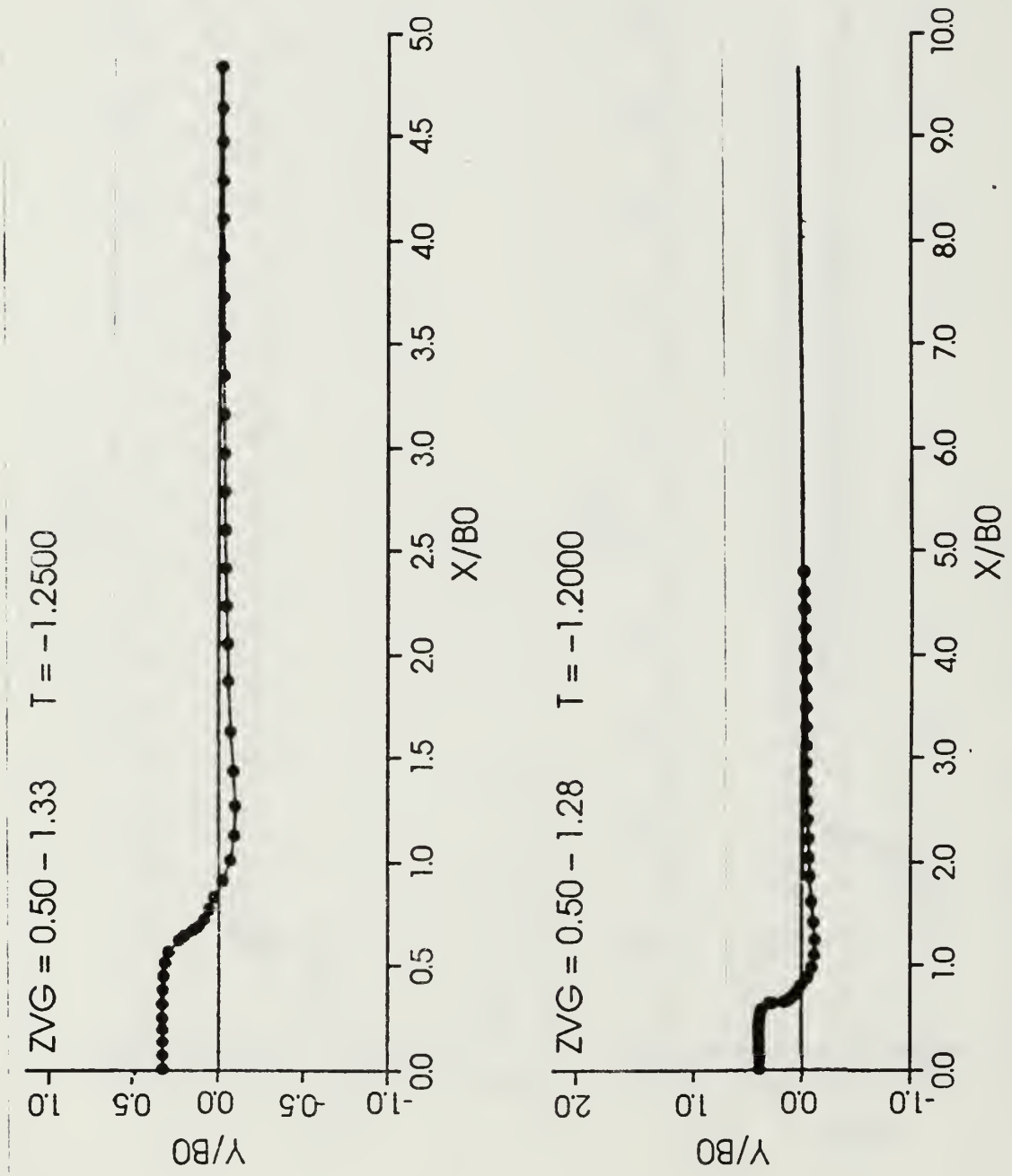

Figure 22. **Run 15, Free Surface Deformation, xv = 0.5**

III. SMOOTHING

A. INTRODUCTION

Despite all efforts to minimize the effect, or delay the onset, of the numerical Helmholtz instabilities during the parametric study, they consistently occur and are clearly inevitable. Extensive efforts were expended to discover an additional parameter within the model that would minimize the effect of the instabilities or delay their formation. During the course of the parametric study, as a path of investigation, it was decided to observe the variation of the circulation strength of the free surface vortices with respect to increasing x/b_0 distance as measured from center line. It was theorized that sharp differences in circulation values between adjacent vortices were responsible for the tendency of the adjacent vortices to rotate about each another.

As a representative sample, run 12 was utilized to depict the variation of the circulation with respect to x/b_0. Figure 23 clearly demonstrates the so called "sawtooth" instabilities. Each point on the figure represents an individual free surface vortex circulation strength.

It is useful to observe the interaction of the Helmholtz instabilities with the variation of the circulation values. Figure 24 depicts the free surface vortices that eventually (within one or two time steps) will lead to the onset of a Helmholtz instability. Figure 25 represents the

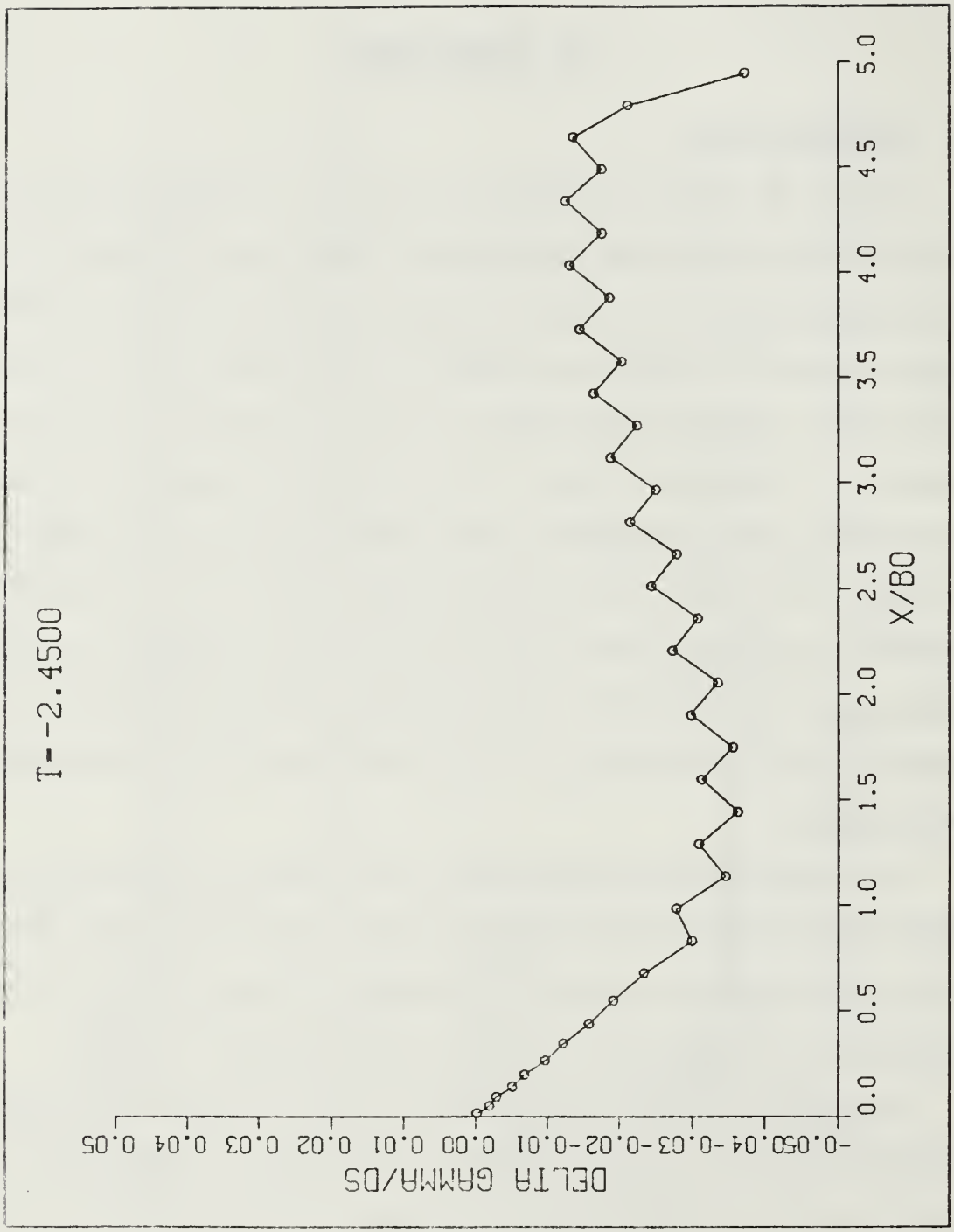

Figure 23. **Run 12, Variation of Γ With Respect to x/b_o**

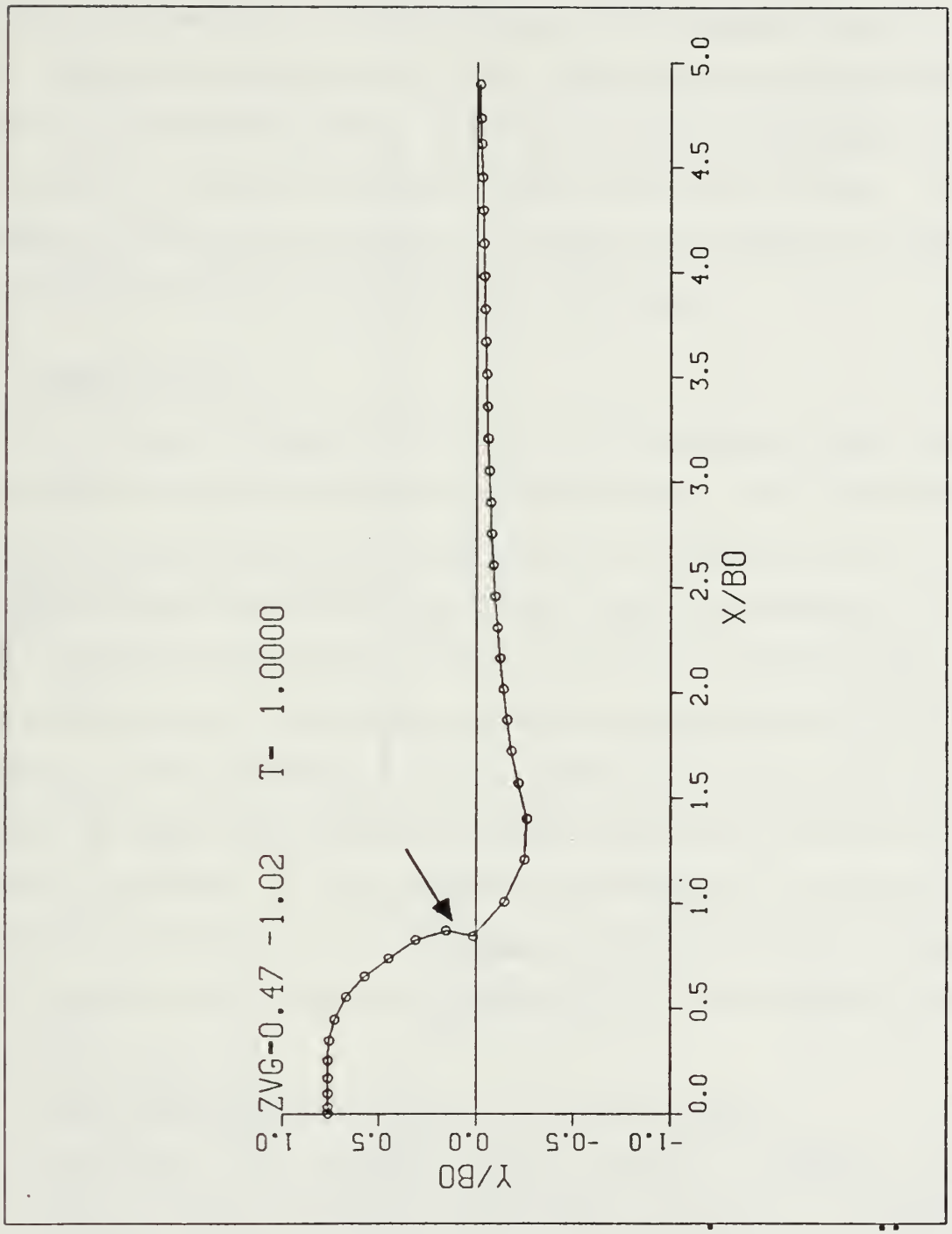

Figure 24. **Run 12, Discrete Vortices Leading to Instabilities**

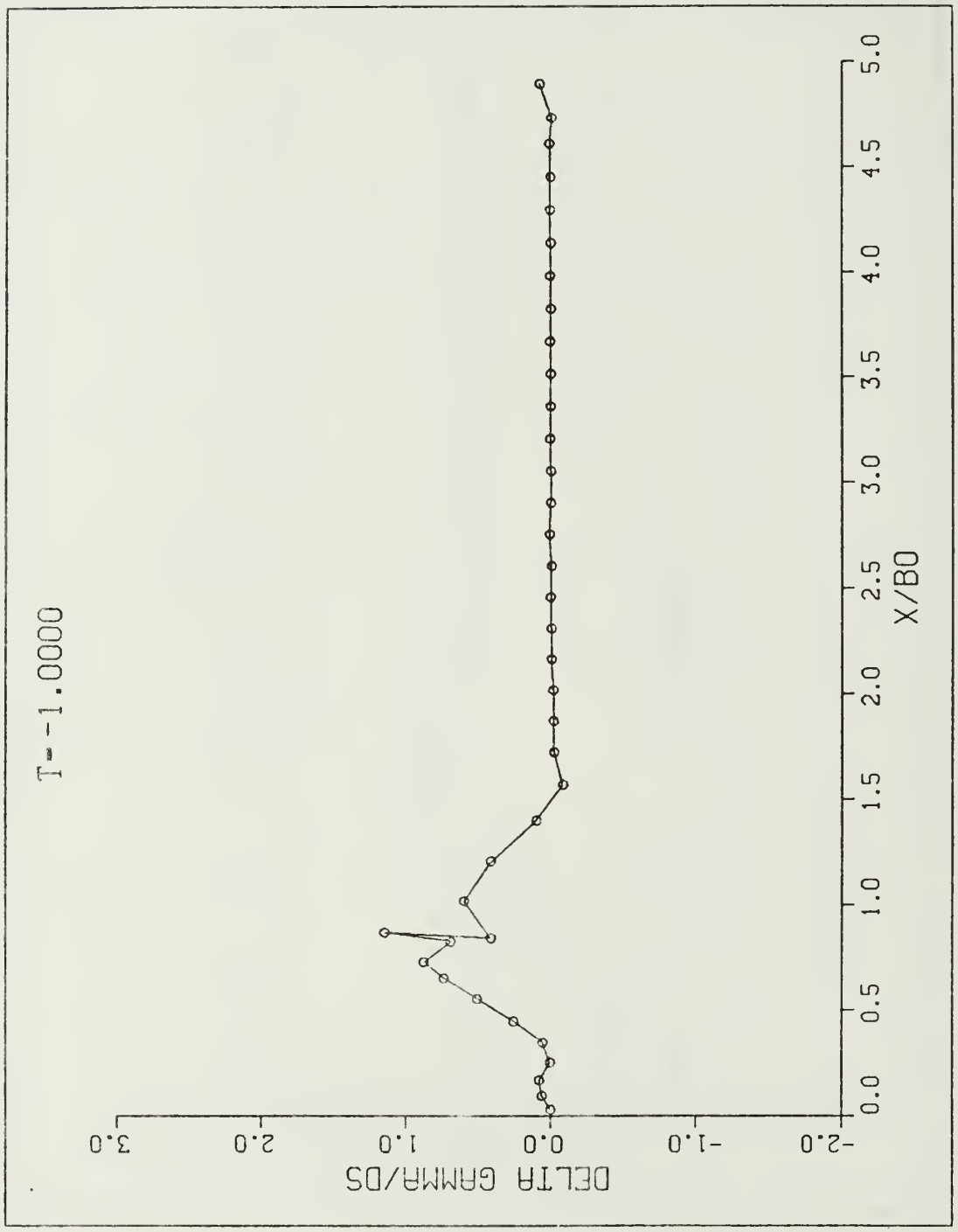

Figure 25. **Run 12, Variation of Γ With Respect to x/b_o**

corresponding value of circulation for each free surface vortex at the time associated with Figure 24. The sharp variation in circulation between the vortices is noted. At the actual point of breakdown, the difference in circulation effectively approaches infinite values. The purpose of attempting to smooth the variation of circulation is to delay the inevitable formation of the Helmholtz instability.

B. APPLICATION

From Longuet-Higgins [Ref 12], a five-point smoothing routine was developed and implemented to smooth the value of the circulation when a set of adjustable parameters have been established and a set of specific conditions have been met. With a minor modification of the code, the operator can elect to either activate the smoothing subroutine continuously or require that a specified condition be met prior to commencing the smoothing routine. Additionally, the operator may specify the exact time where the routine commences looking for the desired conditions. In this particular investigation, the smoothing routine was called when the difference in circulation values between two adjacent vortices was greater than 0.3 and the nondimensional time was at least -2.1.

Other variables that the operator can adjust include:

1. **Start time**. The operator has the ability to specifically state when, in nondimensional time, the smoothing routine is called. Clearly it serves no useful purpose to smooth at early times because the free surface has not started deforming. Since smoothing is an undesirable solution of the problem in any event, its use should be avoided for as long as possible. A nondimensional time of -2.1 was chosen as providing a comfortable margin

of smoothing yet not unnecessarily introducing artificiality into the problem.

2. **Frequency of smoothing**. Once the actual start time of smoothing has been reached, the operator may direct how often future smoothing attempts will be made. Arbitrarily, it was decided that once smoothing started, it would occur every 25 time steps.

3. **Duration of smoothing**. Once smoothing has occurred for a specific time step, the operator may (with a minor modification to the code) elect to automatically smooth the next "N" time steps prior to starting the smoothing counter once again. This selection is useful in that the Longuet-Higgins method is not a dominating technique, and the circulation variation may be so large that it requires several consecutive smoothing time steps to remove the sharp difference which initiated the routine. In this application only, "N" represents the number of consecutive time steps that smoothing will be completed.

4. **X/b_0 position**. It is unnecessary to smooth the variation of the circulation at points along the free surface where instabilities do not exist or normally form. In general, the instabilities form at an x/b_0 range of $(0.5 \leq x/b_0 \leq 1.25)$ at or very close to the formation of the scar.

Figure 26 represents a duplication of run 12 depicted in Figure 23 except with the Longuet-Higgins continuous smoothing routine activated. For this particular run, the following smoothing routine selections were made:

start time:	–2.1
smoothing duration:	five time steps
time delay	25 time steps
x/b_0 range	$0.5 < x/b_0 < 1.25$

Notice that the sharp peak has been reduced yet the basic form of the free surface deformation has been retained.

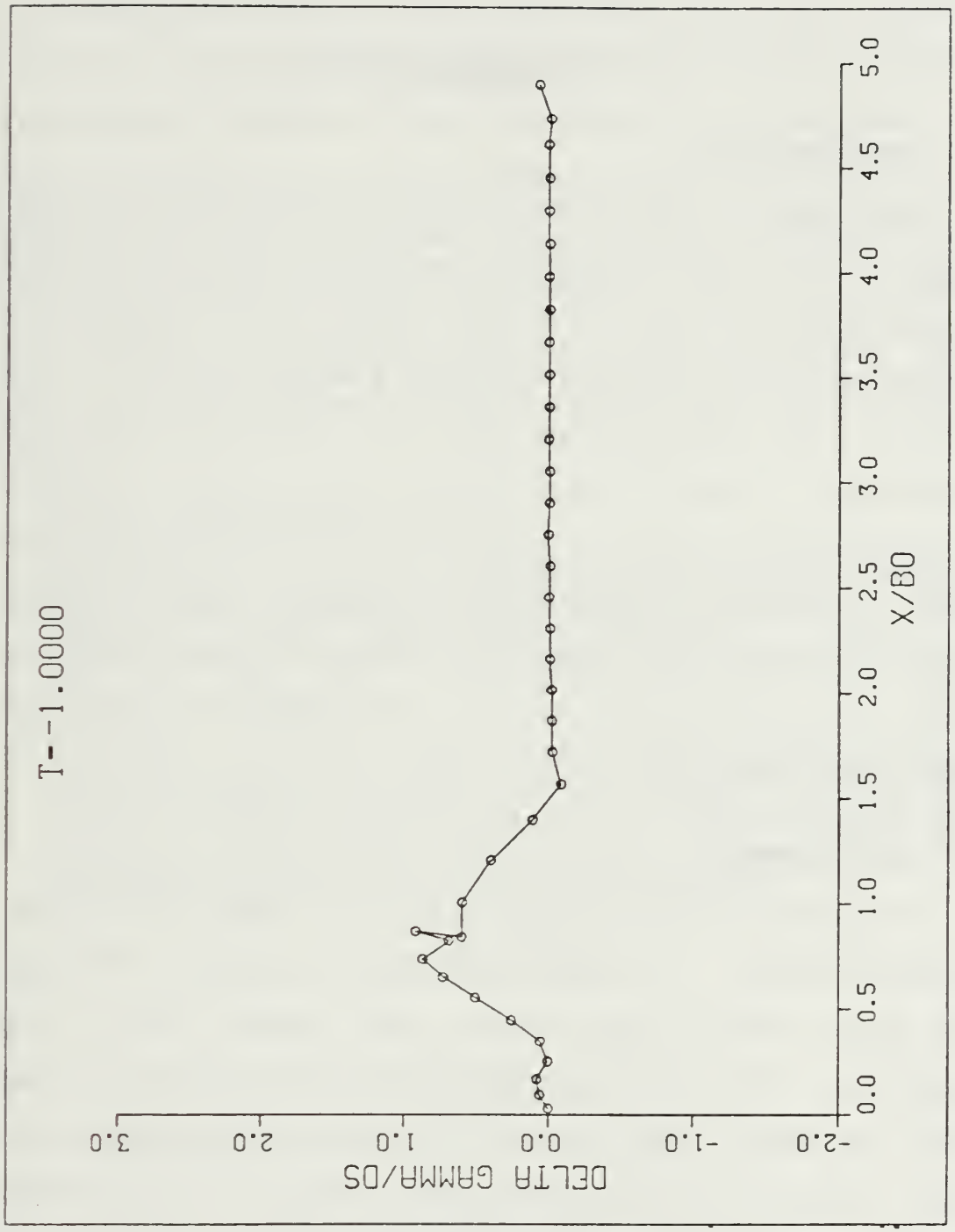

Figure 26. **Run 12, Smoothed Variation of Γ With Respect to x/b_o**

IV. RE-DISCRETIZATION

A. INTRODUCTION

After close scrutiny of each run during this parametric study, it was determined that developing a method of re-discretizing the free surface would be useful. This task required the development of a routine within the model that would add a discrete vortex at a specific location. The critical problem would be to determine exactly when and where to add a free surface vortex element and what corresponding circulation to assign to it. The routine must have the ability to interrupt program execution during any specific time step, make the determination that a new vortex is required, and place it while still maintaining the continuity of the program and the general form of the free surface.

B. APPLICATION

A subroutine was developed within the code and assigned an activation option. If the "add vortex" option is selected, the program will add a discrete free surface vortex element under specific conditions. This routine calculates the complex distances between each free surface vortex element and stores the information in an array. When the difference of the rate of change of distance between two adjacent vortices exceeded an adjustable percentage value, the subroutine "ADDVOR" was called. For the purposes of this investigation, the specific value utilized was 33 percent.

An additional restriction was imposed upon the routine requiring that the two vortices under consideration be increasing the distance between them instead of closing the distance between them. If indeed the distance between two surface vortices was closing at an acceptable rate (i.e., greater than the 33 percent requirement), the subroutine would add vortices at those positions along the free surface. This is obviously undesirable because the vortices are already closely packed. Figure 27 represents a typical situation where a vortex would be added.

Operator considerations include:

1. **Closing rate**. As discussed earlier, the rate of change of distance between vortices will dictate when the program will add a vortex. There is no restriction as to the percentage that is chosen but it was determined that an acceptable range was between 30 percent and 50 percent.

2. **Circulation**. The value of the circulation of the added vortex was calculated algebraically between the two vortices so that the slope of the circulation with respect to x/b_0 would be preserved between the (now) three surface vortices. The values of the new circulations are given by the following expressions:

$$\Gamma_1' = (5*\Gamma_1 - \Gamma_2)/6 \tag{5}$$

$$\Gamma_2' = (5*\Gamma_2 - \Gamma_1)/6 \tag{6}$$

$$\Gamma_{new} = (\Gamma_1 + \Gamma_2)/3 \tag{7}$$

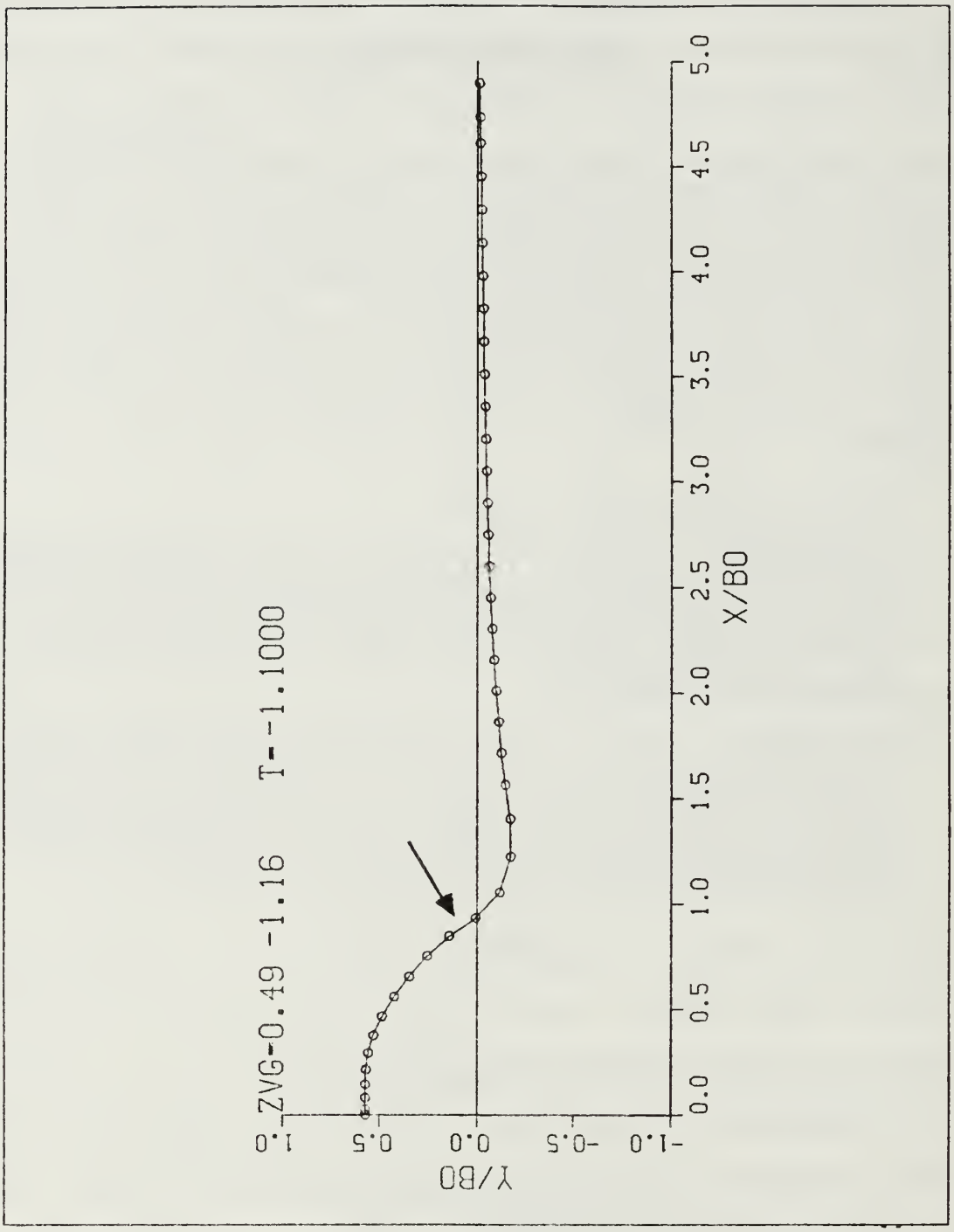

Figure 27. **Typical Free Surface Condition Requiring an Additional Vortex**

Γ_1 represents the circulation of vortex #1 and Γ_2 represents the circulation of vortex #2 prior to the addition of the new vortex. Γ_1' and Γ_2' represent the new calculated vortex circulation values, respectively. Γ_{new} represents the value of the circulation of the new vortex.

3. **New vortex position**. In order to accurately place the new vortex, it was decided to calculate the new Z position utilizing a conservation of circulation principle. Accordingly, the position of the new vortex (Znew) is given by the expression:

$$Znew = \left((\Gamma_1 * z_1 + \Gamma_2 * z_2) - (\Gamma_1' * z_1 + \Gamma_2' * z_2)\right)/\Gamma_{new} \qquad (8)$$

Although several placement and circulation algorithms were developed and tested, the ones listed in equations (5) through (8) performed the most adequately. Figure 28 represents the execution of this routine immediately following the addition of a vortex. This figure follows Figure 27 in time. Notice that the routine placed the vortex in a satisfactory manner. Figure 29 represents the circulation strength assigned to the added vortex.

4. **Smoothing** As can be seen from Figure 29, although the circulation is correctly assigned to the new vortex, there is a slight difference between the new value and the circulation values of its adjacent vortices. Accordingly, the operator may elect to immediately smooth the circulation values after adding a vortex. This may not be necessary, however, if the value of the circulation difference exceeds 0.3 of its neighbors as mentioned earlier. Figure 30 depicts a smoothed version of the circulation strength of the added vortex.

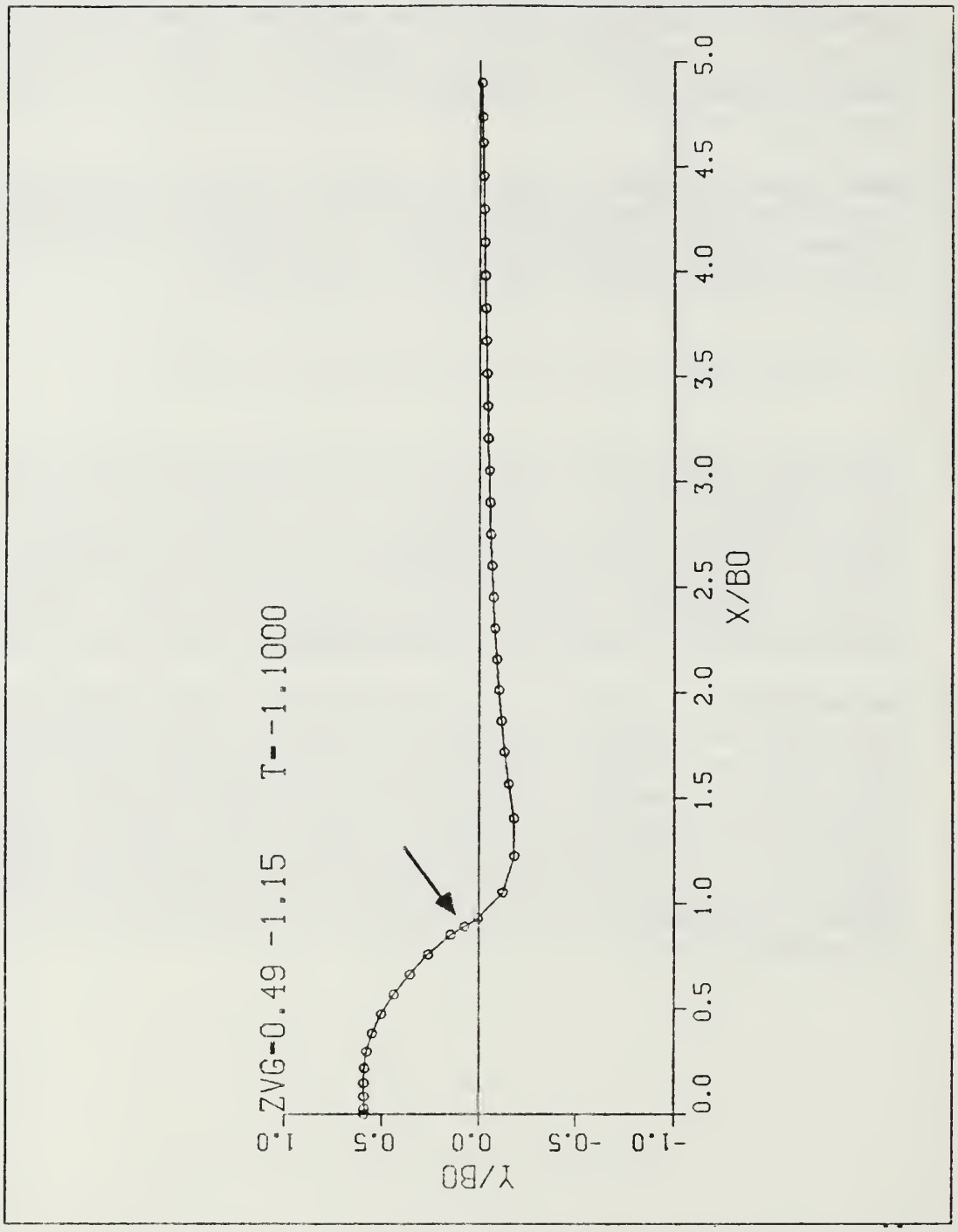

Figure 28. **Free Surface Deformation Immediately After Adding a Vortex**

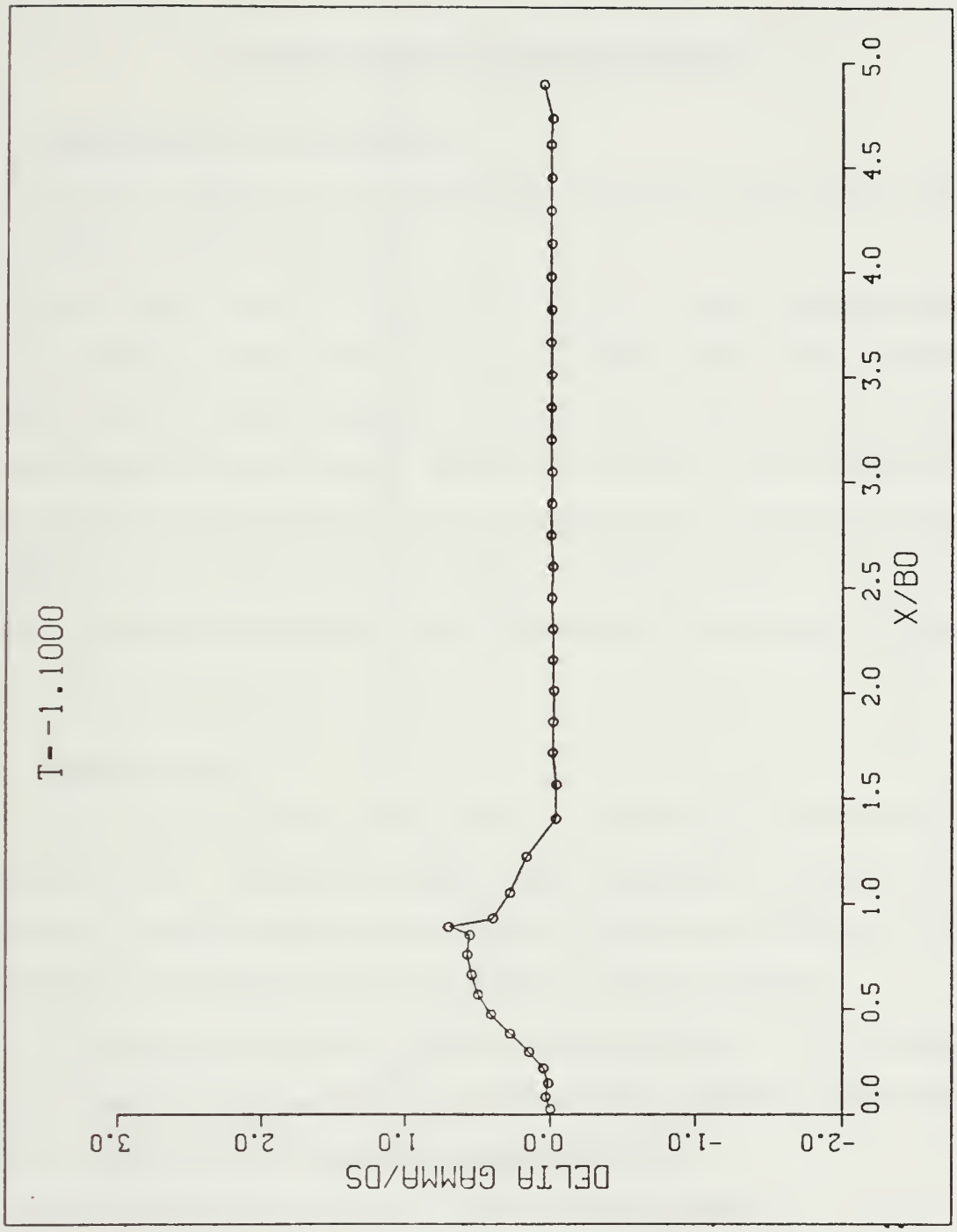

Figure 29. **Circulation Value of an Added Vortex**

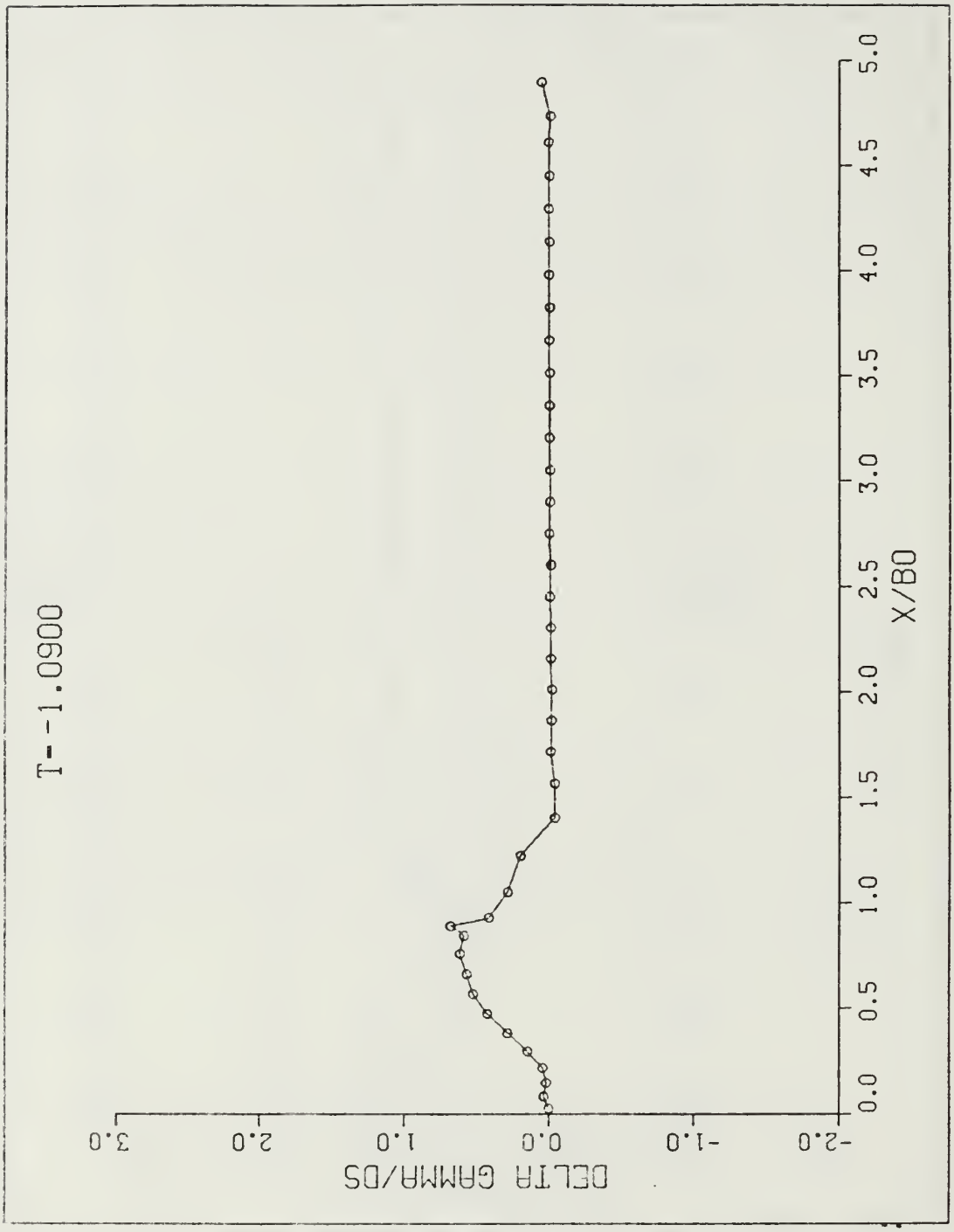

Figure 30. **Smoothed Circulation Value of an Added Vortex**

V. STRATIFIED FLOW EXPERIMENTS

A. EXPERIMENTAL APPARATUS

Specific details of the experimental apparatus were discussed extensively by Leeker [Ref 11].

Experiments were conducted in a water basin approximately twelve feet long, three feet wide, and four feet deep. Two counter-rotating vortices were generated through the use of two opposing plates activated by a system of weights and pulleys. Flow visualization was performed through the use of a fluorescene dye injected through openings on the underside of each plate. A video camera, a VHS video cassette recorder, a monitor, and a date/timer were utilized as supplementary equipment.

B. PROCEDURES

Basic experimental procedures were thoroughly discussed by Leeker [Ref 11]. The procedures in this investigation, although fundamentally similar, differed from those of Leeker with respect to the addition of a sharp salt-water/fresh-water density interface.

To obtain a sufficiently sharp density difference, 50 pounds of ordinary salt were thoroughly mixed with 465.7 gallons of fresh water in the tank bottom and allowed to settle overnight.

From Striftos [Ref 14], the concentration is given by:

$$1/C = 1 + \frac{\text{weight [water]}}{\text{weight [salt]}} \tag{9}$$

The density of the salt water layer is given by the expression:

$$\rho_s = \rho_o * (1 + .71 * C) \qquad (10)$$

Where ρ_o is the density of the fresh water (62.43 lbs/ft^3).

The density difference then is simply given by $(\rho_s - \rho_o)$. For the purposes of these experiments, C = .0127 lbs. salt/lbs. water, and ρ_s = 62.993 lbs./ft^3. Finally, $\Delta\rho$ =.563 lbs./ft^3.

A freshwater dye combination was introduced by gravity feed from a reservoir through small tubes which spilled onto a floating board in the tank. The dyed freshwater trickled over the edge of the board and settled on top of the salt-water layer. The tank was filled in this manner for several hours, resulting in a sharp density interface. The remainder of the experiments were carried out in the normal method. Efforts were concentrated on recording the interaction of the vortex pair with the interface.

C. RESULTS OF THE EXPERIMENTAL RUNS

Approximately ten experimental runs were completed. Two runs (04 02 and 04 08) were chosen to discuss as representative samples. Analysis procedures of all experimental runs were identical to those discussed by Leeker [Ref 11].

Figure 31 depicts the right vortex (and image) center's path for run 04 02. Figure 32 depicts the nondimensional velocity profile of the right vortex center also for run 04 02. Based on the maximum velocities displayed by Figure 32, the Froude number for the vortex in saltwater = 0.78 and for freshwater = 1.05.

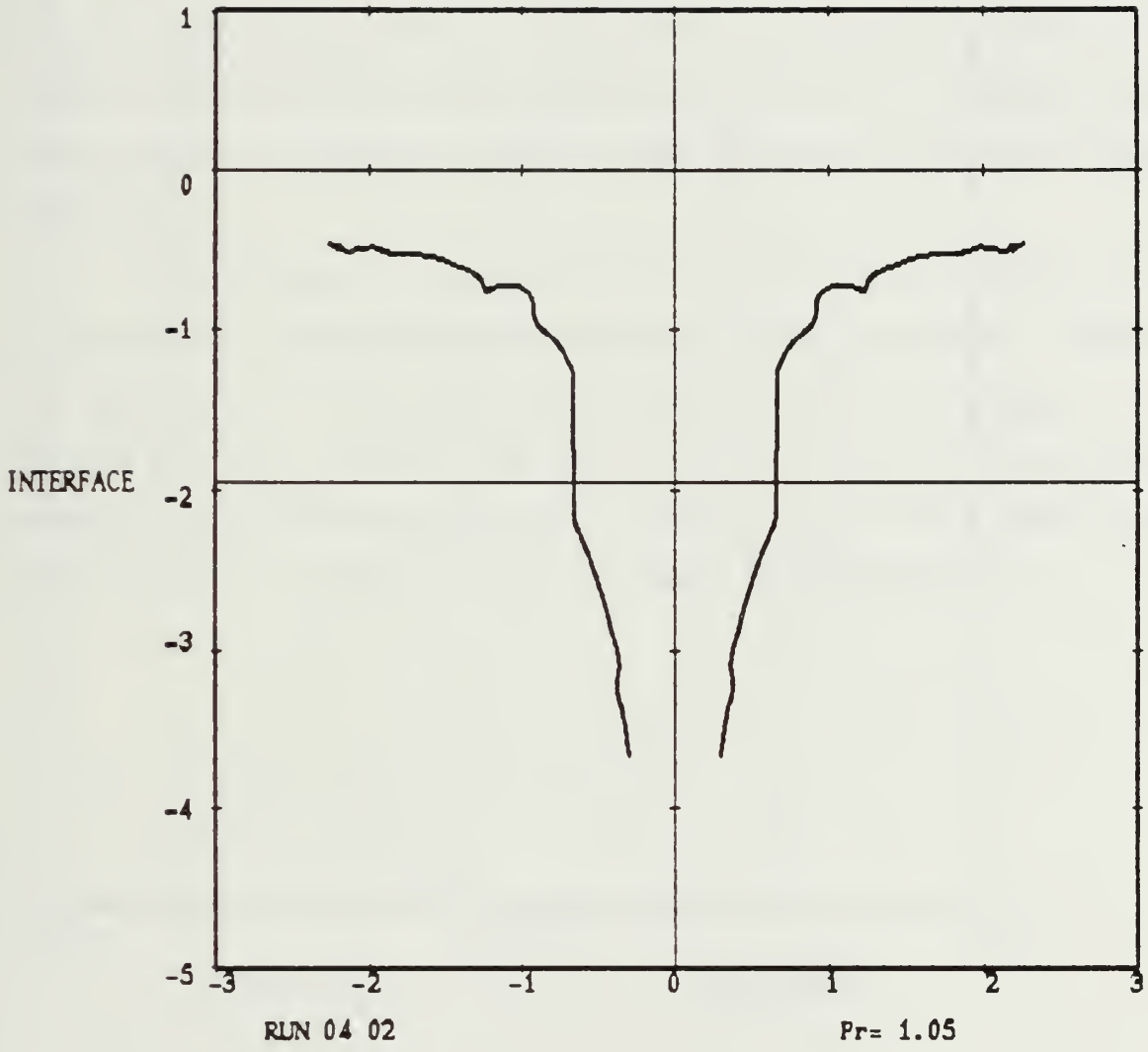

Figure 31. **Vortex Center Path for Run 04 02, Fr = 1.05**

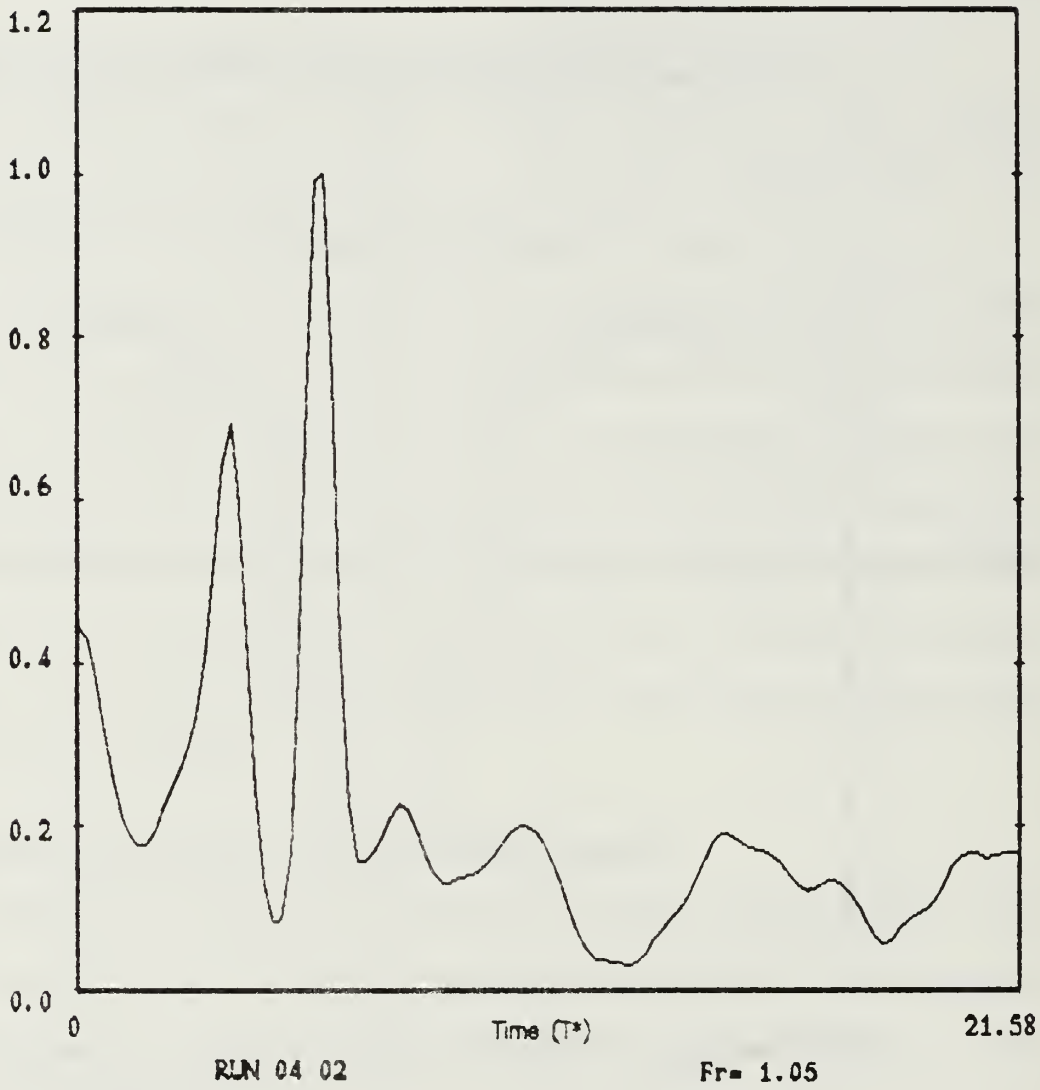

Figure 32. **Vortex Center Nondimensional Velocity for Run 04 02, Fr = 1.05**

From Figure 31, the vortex center clearly "saw" the density interface as a makeshift free surface and began to deflect. Upon intrusion into the lower-density fluid, the velocity increased and the vortex path became more vertical; in effect, the vortex no longer "saw" a barrier. As the vortex center is influenced by the actual free surface, it behaved much like previous investigations [Refs 10, 11]. The two distinctly different maximum velocity peaks on Figure 32 support this observation.

The vortex in run 04 08 was only visible while in the lower salt-water layer. Figure 33 depicts the vortex and image path. Figure 34 represents the nondimensional velocity profile of the vortex center. In this run, although the center was not tracked through the interface, the vortex also appeared to "see" that there was a slight free surface above it, as evidenced by the outward slant of its path.

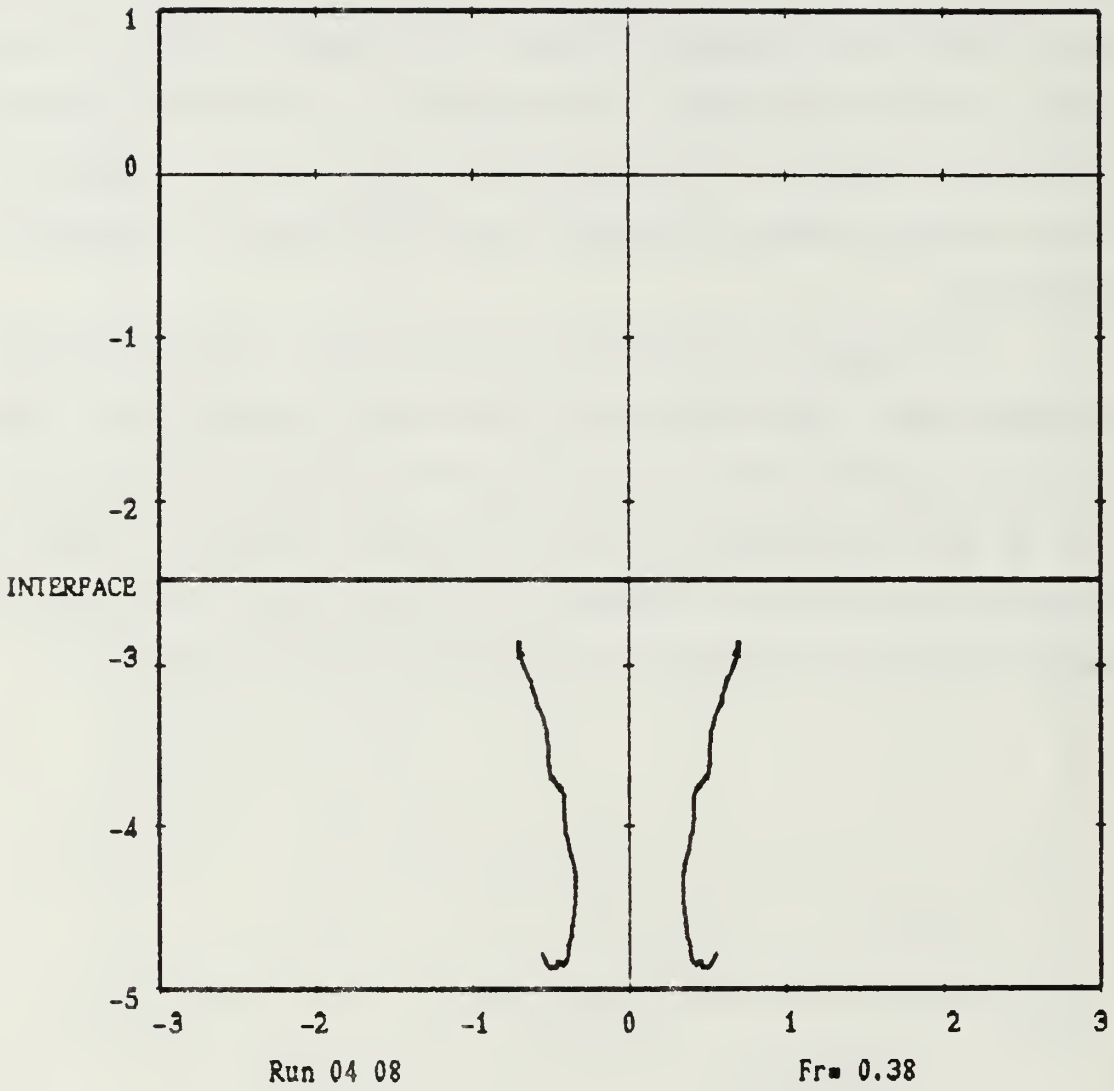

Figure 33. **Vortex Center Path for Run 04 08, Fr = .38**

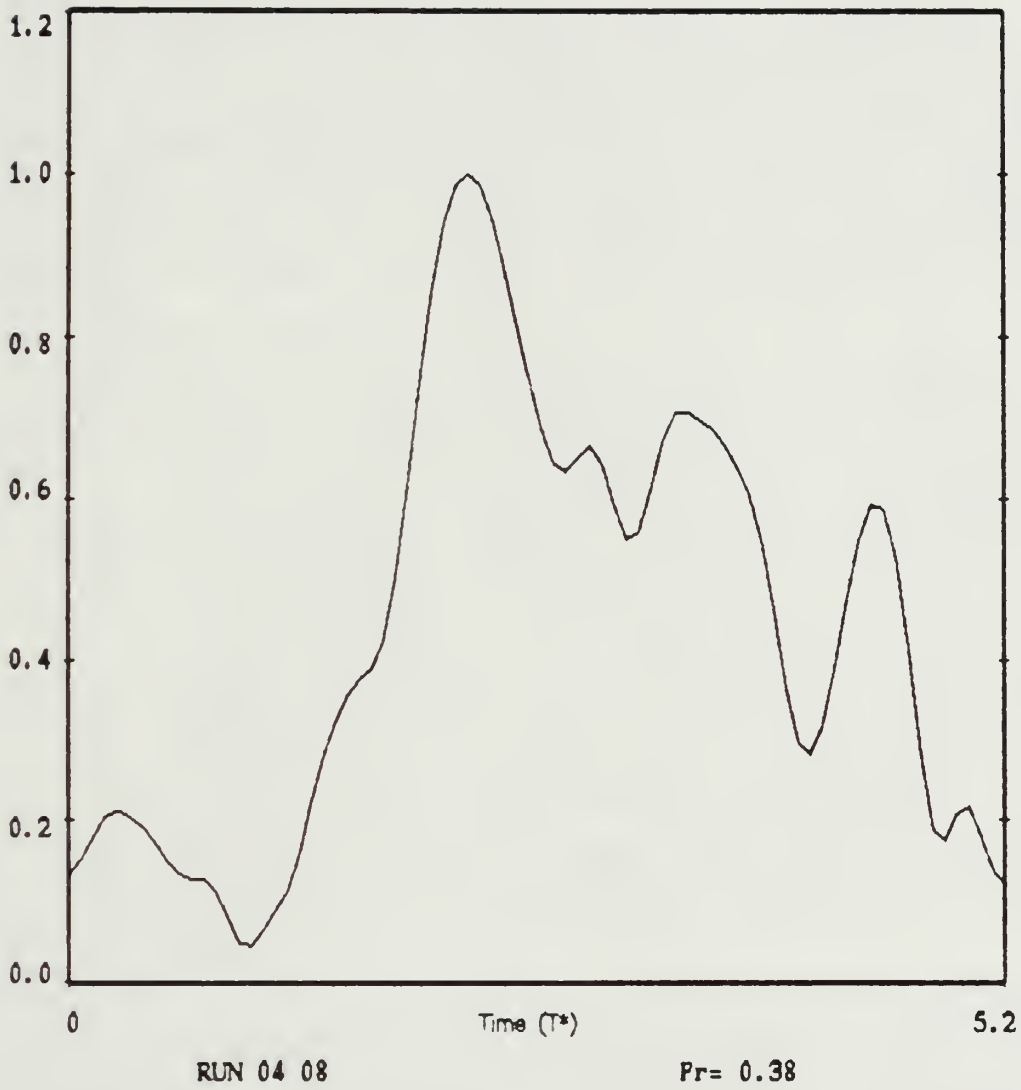

Figure 34. **Vortex Center Nondimensional Velocity for Run 04 08, Fr = .38**

VI. CONCLUSIONS

The numerical analysis has shown that the evolution of the free surface can be calculated through the use of the line vortices. No filtering is necessary provided that the complex velocity function is desingularized in a suitable manner. The analysis becomes more robust as the Froude number is increased. Even then, the inception of small-wavelength Helmholtz instability cannot be avoided. However, the time at which such instabilities occur can be delayed by a suitable arrangement of the initial position of the vortices. Fortunately, however, the critical time at which the instability manifests itself is near the time at which the wave breaking is likely to occur. This analysis is not equipped to deal with wave breaking. For smaller Froude numbers (say Fr = 0.50), the agreement between the calculated and measured free surface shapes is quite encouraging. A better agreement would have been a source of puzzlement rather than a source of gratification because the vortices in the experiments become quickly turbulent, diffuse over a large area and lose their strength due to the cancellation of oppositely signed vorticity in the overlapping regions of vortices and due to the negative vorticity generated at the free surface. Although the numerical model has the capability to vary the vortex strength with time (e.g., using a diffusing Oseen vortex), this was not done.

For any of the Froude numbers encountered in the analysis or experiments, no wave train was observed on either side of the scars. This conclusion was somewhat anticipated on the basis of previous calculations. For very small Froude numbers (say, Fr < 0.15), the scars were very small, the vortices followed the rigid-wall path, and the scars were slaved to the vortices, as found previously by Sarpkaya and Henderson [9].

The numerical model can be improved, within the limitations of the inviscid flow theory, by using vortex sheet panels rather than line vortices. It is also possible to use an adaptive grid system together with a suitable finite-difference method to solve the equations of motion directly. Nevertheless, the difficulties stemming from the occurrence of Helmholtz instability during the roll-up of the vortex sheets, axial instability of the vortex pair, three-dimensional instabilities on the free surface and the turbulent diffusion of the vortices remain as the most serious impediments towards an exact solution of the problem.

In summary, the principal objectives of this investigation have been accomplished. The extensive parametric study has shown that the numerical model is relatively insensitive to a variety of changing parameters and that the Helmholtz instabilities are inevitable in the execution of this code beyond some critical time.

The supplementary objective of analyzing the interaction of a vortex pair with a sharp density interface was also accomplished.

Although only a preliminary to major investigations in the future, this "first look" of the interaction of two counter-rotating vortices with a sharp density interface revealed interesting information, such as the considerable increase in velocity of the vortex pair after its intrusion into the fresh-water layer.

LIST OF REFERENCES

1. Naval Postgraduate School, Monterey, CA, NPS-69-82-003, *Trailing Vortices in Stratified Fluids*, by T. Sarpkaya, and S. K. Johnson, June 1982.

2. Johnson, S. K., *Trailing Vortices in Stratified Fluids*, M.S. Thesis, Naval Postgraduate School, Monterey, CA, December 1982.

3. Turkmen, C., *Trailing Vortices in Stratified and Unstratified Fluids*, M.S. Thesis, Naval Postgraduate School, Monterey, CA, December 1982.

4. Gray, W. E., *Scars on Striations Due to Trailing Vortices*, M.S. Thesis, Naval Postgraduate School, Monterey, CA, March 1985.

5. Daly, J. J., *Effects of Ambient Turbulence and Stratification on the Demise of Trailing Vortices*, M.S. Thesis, Naval Postgraduate School, Monterey, CA, March 1986.

6. Noble, W. D., *Characteristics of Vortices in Stratified Media*, M.S. Thesis, Naval Postgraduate School, Monterey, CA, September 1986.

7. Miller, B. S. L., *Vortex Motion in a Stratified Medium*, M.S. Thesis, Naval Postgraduate School, Monterey, CA, December 1986.

8. Striftos, C., *Vortex Motion in Stratified Fluids*, M.S. Thesis, Naval Postgraduate School, Monterey, CA, March 1982.

9. AIAA Paper No. AIAA-85-0445, *Free Surface Scars and Striations Due to Trailing Vortices Generated by a Submerged Lifting Surface*, by T. Sarpkaya and D. O. Henderson, January 1985.

10. Elnitsky, J. II, *Interaction of a Vortex Pair With a Free Surface*, M.S. and M.E. Thesis, Naval Postgraduate School, Monterey, CA, September 1987.

11. Leeker, R. E., *Free Surface Scars due to a Vortex Pair*, M.S. Thesis, Naval Postgraduate School, Monterey, CA, March 1988.

12. Rosenhead, L., "The Spread of Vorticity in the Wake Behind a Cylinder," *Proceedings of the Royal Society of London*, Series A., v. 127, 1930, pp. 590–612.

13. Longuet-Higgins, M. S. and E. D. Cokelet, "The Deformation of Steep Surface Waves on Water," *Proceedings of the Royal Society of London*, v. 350, 1976, pp. 1–26.

14 Striftos, C., *Vortex Motion in Stratified Fluids*, M.S. Thesis, Naval Postgraduate School, Monterey, CA, March 1982.

INITIAL DISTRIBUTION LIST

		No. Copies
1.	Defense Technical Information Center Cameron Station Alexandria, VA 22304–6145	2
2.	Library, Code 0142 Naval Postgraduate School Monterey, CA 93943-5002	2
3.	Department Chairman, Code 69 Department of Mechanical Engineering Naval Postgraduate School Monterey, CA 93943-5000	1
4.	Professor T. Sarpkaya, Code 69SL Department of Mechanical Engineering Naval Postgraduate School Monterey, CA 93943-5000	10
5.	LT Richard E. Leeker, Jr. 3028 Autumn Shores Drive Bridgeton, MO 63044	1
6.	LT Mark D. Petersen-Overton 713 Clearview Drive Charleston, SC 29412	1
7.	Commanding Officer David Taylor R & D Center Carderrock Laboratory Bethesda, MD 20084	1
8.	Naval Sea Systems Command PMS 350 Washington, D. C. 20362	1

Thesis
P396 Petersen-Overton
c.1 The interaction of a
fluid interface with a
vortex pair.